1   **Evaluating Secondary Inorganic Aerosols in 3-Dimensions**
2
3   **Keren Mezuman**[1,2], **Susanne E. Bauer**[3,2,*], **Kostas Tsigaridis**[3,2]
4   [1]Earth and Environmental Sciences, Columbia University, New York, NY, USA
5   [2] NASA Goddard Institute for Space Studies, New York, NY, USA
6   [3] Center for Climate Systems Research, Columbia University, New York, NY, USA
7   * To whom correspondence should be addressed, susanne.bauer@columbia.edu
8
9   **Abstract.**

10   The spatial distribution of aerosols and their chemical composition dictates whether aerosols

11   have a cooling or a warming effect on the climate system. Hence, properly modeling the 3-

12   dimensional distribution of aerosols is a crucial step for coherent climate simulations. Since

13   surface measurement networks only give 2-D data, and most satellites supply integrated

14   column information, it is thus important to integrate aircraft measurements in climate model

15   evaluations. In this study, the vertical distribution of secondary inorganic aerosol (i.e. sulfate,

16   ammonium and nitrate) is evaluated against a collection of 14 AMS flight campaigns and

17   surface measurements from 2000-2010 in the USA and Europe. GISS ModelE2 is used with

18   multiple aerosol microphysics (MATRIX, OMA) and thermodynamic (ISORROPIA II, EQSAM)

19   configurations. Our results show that the MATRIX microphysical scheme improves the model

20   performance for sulfate, but that there is a systematic underestimation of ammonium and

21   nitrate over the USA and Europe in all model configurations. In terms of gaseous precursors,

22   nitric acid concentrations are largely underestimated at the surface while overestimated in the

23   higher levels of the model, influenced by strong stratosphere-troposphere exchange.

24   Heterogeneous reactions on dust surfaces is an important sink for nitric acid, even high in the

25   troposphere. At high altitudes, nitrate formation is calculated to be ammonia limited. The

26   underestimation of ammonium and nitrate in polluted regions is most likely caused by a too

Atmospheric
Chemistry
and Physics
Discussions

27 simplified treatment of the NH_3/NH_4^+ partitioning which affects the HNO_3/NO_3^- partitioning.

28 **1. Introduction**

29 The impact of aerosols on climate and air quality is a function of their chemical composition,

30 abundance and spatial distribution. Understanding the vertical profile of aerosols is crucial for

31 radiative forcing calculations (Xu and Penner, 2012), since aerosols interact with radiation

32 directly through absorption and scattering (Bauer and Menon, 2012; Haywood and Boucher,

33 2000; Stocker et al., 2013), and indirectly via interactions with clouds (Lohmann and Feichter,

34 2005). Comparisons of model results with organic aerosol aircraft data showed large

35 discrepancies in the free troposphere (Heald et al., 2005, 2011). Sulfate and ammonium nitrate

36 aerosols, although much simpler to model than organics, have not been studied in the vertical

37 in much detail. There is large uncertainty in the magnitude of the forcing induced by sulfate and

38 ammonium nitrate aerosols, with estimates for the preindustrial to present day direct radiative

39 forcing of sulfate ranging from -0.6 to -0.2 Wm^{-2} while for ammonium nitrate from -0.3 to -0.03

40 Wm^{-2} (Stocker et al., 2013) under present day conditions. These forcings are projected to

41 change in the future, driven by trends in precursor emissions. The projected increase in

42 agricultural ammonia emissions, which will result in greater availability of ammonia, contrasted

43 with the projected reductions in NO_x emissions, can lead to an increased relative contribution

44 of ammonium nitrate to the total secondary inorganic aerosol (SIA) abundance, due to the

45 strong projected decrease of sulfate aerosols (Hauglustaine et al., 2014; Hodas et al., 2014).

46 Yet, the effect of these changes on ammonium nitrate concentrations are still a matter of active

47 research: *Paulot et al.* [2016] showed increases in nitrate load in the free troposphere, while

48 surface concentrations decreased, and *Pusede et al.* [2016] showed changes in tropospheric

Atmospheric
Chemistry
and Physics
Discussions

49   chemistry in western USA, with increased ammonium nitrate production during daytime rather

50   than at night.

51   Thermodynamically, ammonia tends to neutralize sulfuric acid over the highly volatile nitric acid

52   (Tagaris et al., 2007). The formation of fine-mode nitrate is a function of ammonia, sulfate

53   availability and relative humidity (RH), since its precursor, nitric acid, condenses following

54   thermodynamic equilibrium (Potukuchi and Wexler, 1995a, 1995b). Sulfuric acid and nitric acid

55   also participate in heterogeneous uptake on dust particles, forming coarse sulfate and nitrate, a

56   process that acts as a sink for the gas phase precursors (Bauer and Koch, 2005; Ravishankara,

57   1997).

58   In this paper we evaluate ammonium, nitrate and sulfate aerosols in the NASA GISS ModelE2

59   against surface and aircraft observations, extending what *Bauer et al.* [2007b] did for nitrate

60   aerosol for the year 2000, by using new aerosol configurations that had been implemented in

61   GISS ModelE2 since then, and a substantially extended record of SIA measurements, both from

62   ground stations and various flight campaigns. To assess the model in terms of SIA surface

63   distribution and vertical profiles, we evaluated the performance of three aerosol

64   configurations, described in section 2.1.1, by comparing them against surface data measured

65   over the USA and Europe during 2000-2010, and 14 flight campaigns, as described in section

66   2.2. We then study the climatology of the model against measurements, both at surface and at

67   higher altitudes (sections 3.1-3.3), and explore the model uncertainties with the help of

68   sensitivity experiments (section 3.4).

69   **2. Experimental approach**

Atmospheric
Chemistry
and Physics
Discussions

2.1 Model description

71 The NASA GISS ModelE2 model (Schmidt et al., 2014) was run with interactive tropospheric

72 (Shindell et al., 2001, 2003) and stratospheric chemistry (Shindell et al., 2006) and coupled with

73 three different aerosol configurations, as described below. A horizontal resolution of 2° in

74 latitude by 2.5° in longitude and a vertical resolution of 40 layers to 0.1 hPa was used. The

75 simulation was nudged using 6 hourly National Centers for Environmental Prediction (NCEP)

76 reanalysis data (Kalnay et al., 1996) for the horizontal wind component. Sea surface

77 temperatures (SSTs) and sea ice cover were prescribed using the Met Office Hadley Center's sea

78 ice and sea surface temperature data set (HadISST1) (Rayner et al., 2003).

79 The nitrate optical depth of GISS ModelE2 in the CMIP5 archive was found to be problematic,

80 consistent with the findings of *Shindell et al.* [2013] for a likely too high nitrate load. In our work

81 the nitrate scheme had been corrected and nitrate distribution in the column reflects surface

82 sources such as agricultural, industrial and biomass burning areas.

2.1.1 Aerosols schemes

84 Two aerosol schemes were used in this study: OMA (One Moment Aerosol) (Koch et al., 2006;

85 Miller et al., 2006) and MATRIX (Multiconfiguration Aerosol TRacker of mIXing state) (Bauer et

86 al., 2008). OMA is a bulk mass scheme with one fine mode bin of prescribed size for SO_4^{2-}, NH_4^+,

87 and NO_3^-. In OMA, heterogeneous uptake of SO_2 and HNO_3 on dust surfaces is also included,

88 which takes place on the three smallest size bins out of the five size bins used for mineral dust

89 (Bauer et al., 2004, 2007). MATRIX is a microphysical scheme representing nucleation,

90 condensation and coagulation. Sulfate is tracked with both number and mass concentrations

91 for 16 populations, which are based on mixing state. MATRIX represents an intermediate level

Atmospheric
Chemistry
and Physics
Discussions

92   of complexity; only the total mass of nitrate, ammonium and aerosol water is calculated, and

93   then distributed across populations based on the sulfate abundance in each one of them,

94   assuming internally mixed components. This approach greatly reduces the required number of

95   transported variables.

96   Due to the focus on SIA in this paper we will give a brief description of the sulfate and nitrate

97   schemes in our model. The sulfate chemistry module in both schemes, OMA and MATRIX, is

98   based on Koch et al. (1999) and includes prognostic calculation of gas and aqueous phase DMS,

99   MSA, SO_2 and sulfate concentrations. This provides the sulfate mass in the OMA scheme, and

100   provides aqueous sulfate production rates and H_2SO_4 concentrations as input parameters for

101   MATRIX microphysics (Bauer et al., 2008).

102   To partition between the gas and particle phases the model uses the non-linear

103   thermodynamics. Both schemes were run coupled to the secondary inorganic aerosol

104   thermodynamics scheme EQSAM (Metzger et al., 2002a, 2002b). MATRIX was also run coupled

105   to ISORROPIA II (Fountoukis and Nenes, 2007), which was only recently introduced into GISS

106   ModelE2. EQSAM is a parameterized thermodynamics scheme that relies on the relationship

107   between activity coefficients and RH to calculate the solute activity and the non-ideal solution

108   properties, while ISORROPIA II calculates the equilibrium constants and solves the

109   thermodynamic equations analytically. Both models use the same input parameters: NH_x

110   ($NH_3 + NH_4^+$), SO_4^{2-}, XNO_3 ($HNO_3 + NO_3^-$), RH and temperature, and interactively calculate the SO_4^{2-}

111   , NH_4^+, NO_3^- and aerosol H_2O concentrations at equilibrium, as well as the residual NH_3 and

112   HNO_3 in the gas phase.

113   The thermodynamical equilibrium for Aitken mode sized particles, which is important for CCN,

Atmospheric
Chemistry
and Physics
Discussions

Open Access

EGU

114   might not be properly captures by models (*Benduhn et al.* [2016]). This is not expected to be a

115   problem in this study because Aitken mode particles are a small fraction of the total aerosol

116   mass. In addition, for the coarse mode, large uncertainties exist regarding the availability of

117   crustal and coarse mode material in equilibrium thermodynamic calculations. Our simulations

118   do not take into consideration crustal (e.g. Mg^{2+}, K^+, Ca^{2+}) and sea salt (e.g. Na^+, Cl^-) ions in the

119   thermodynamics, although this option is available in the model.

120   The model ran in the following three configurations: OMA-EQSAM, MATRIX-EQSAM, and

121   MATRIX-ISORROPIA, and we are comparing model $PM_{2.5}$ (particles with dry diameter smaller

122   than 2.5 μm) with measured $PM_{2.5}$ at surface, and model PM_1 (particles with dry diameter

123   smaller than 1 μm) with measured PM_1 at the vertical, for consistency with the available

124   measurements.

125   **2.1.2 Emissions**

126   This study used the Coupled Model Intercomparison Project phase 5 (CMIP5) historical

127   anthropogenic emissions until 2005 (Lamarque et al., 2010) and the Representative

128   Concentration Pathway 4.5 (RCP4.5) scenario thereafter (van Vuuren et al., 2011). Biomass

129   burning emissions came from the Global Fire Emissions Database (GFED3) inventory (van der

130   Werf et al., 2010). The emissions include seasonal variations for the biomass burning, soil NO_x,

131   shipping and aircraft sectors (Lamarque et al., 2010), yet lack seasonal variability for all other

132   anthropogenic emissions, including agricultural NH_3 sources. In order to prevent unrealistic

133   ammonium and nitrate aerosols loads during wintertime, the agricultural NH_3 emissions were

134   altered using the local solar zenith angle, in order to produce a more realistic seasonal

135   variability, but kept the total annual emissions the same. This approach is comparable to *Adams*

Atmospheric
Chemistry
and Physics

Open Access

EGU

Discussions

136   *et al.* [1999] and *Park* [2004] who scaled ammonia emissions from crops and fertilizers

137   according to the number of daylight hours.

138   **2.1.3 Sensitivity runs**

139   NH_3 emissions are controlled by the agricultural sector (Lamarque et al., 2010), both in the USA

140   and Europe, where more than 80% of NH_3 emissions are agriculture-related (van Damme et al.,

141   2015; Paulot et al., 2014). We test how changing agricultural NH_3 emissions affect ammonium

142   nitrate formation under two scenarios: double and five times higher agricultural NH_3 emissions,

143   using the MATRIX-ISORROPIA aerosol configuration. The results of that sensitivity are presented

144   in section 3.4.

145   **2.2 Observational datasets**

146   **2.2.1 Surface measurements**

147   We evaluate our simulations against nitrate and sulfate $PM_{2.5}$ data measured by the

148   Interagency Monitoring of Protected Visual Environments (IMPROVE) network over the

149   continental United States (Malm et al., 1994, 2004), and against ammonia, ammonium, nitric

150   acid, nitrate, SO_2 and sulfate measured by the European Monitoring and Evaluation Programme

151   (EMEP), available via the NILU-EBAS database, for the years 2000-2010. From EMEP we use the

152   corrected sulfate for sea salt (XSO_4) (EMEP, 2014, Chp. 3) as it better represents fine sulfate.

153   IMPROVE currently has 212 sites, predominantly rural (Hand et al., 2011, 2012), while EMEP has

154   around 40 sites measuring aerosol composition in Europe, many of which are urban (Tørseth et

155   al., 2012). The data in Europe is reported in $\mu gX\ m^{-3}$ (where X is either sulfur or nitrogen) and in

156   the USA in $\mu g\ m^{-3}$. We decided to keep these units unchanged in the rest of the manuscript, and

157   convert the units of the model to represent those of the measurements, rather than doing the

158   opposite. We compared monthly mean values from all available stations with monthly mean

159   model output. An examination of the mean spatial distribution over the USA (Figure 1) revealed

160   distinct regimes with different pollution levels, which motivated a regional division of the data

161   into eastern USA (EUSA) and western USA (WUSA). Europe (EU; Figure 2) and the Arctic (ARC;

162   data from flight campaigns only) were studied independently (Table 1). The standard deviation,

163   correlation coefficient (R), and normalized mean bias (NMB) between the monthly mean

164   surface values within the studied regions (black frames in Figures 1 and 2) and the model's

165   monthly mean at the stations locations in each region, were calculated. It is important to note

166   that during the 11-year period the number of measuring sites has varied in each region, and

167   that not all stations measured all species.

168   **2.2.2 Flight campaigns**

169   The Aerodyne Aerosol Mass Spectrometer (AMS), which measures chemical composition and

170   size distribution of non-refractory particles (such as ammonium, nitrate and sulfate) with

171   diameter smaller than 1 μm (Allan et al., 2003; Jimenez et al., 2003), had been part of many

172   flight campaigns in the past decade. Another common method to measure inorganic particle

173   composition is using the particle-into-liquid-sampler (PILS), which quantifies the ionic content

174   of particulate matter using ion chromatography (Weber et al., 2001). In this study we use data

175   from 14 flight campaigns, two of which used the PILS instrument for chemical composition

176   measurements, and the rest used the AMS (Table 2). The flights took place in the Northern

177   Hemisphere during short campaign periods, predominantly during spring and summer seasons,

178   between 2001-2011. The flight tracks of the campaigns used here are presented in Figure 3.

179   Data were retrieved using the Tools for Airborne Data interface (https://tad.larc.nasa.gov/), as

180   well as the AMS global database (https://sites.google.com/site/amsglobaldatabase/). For every

181   campaign a mean regional vertical profile was calculated by averaging the flight data within the

182   model's grid. For short-range campaigns such as ACE, CRISTAL, MILAGRO, TexAQS, and EUCAARI

183   all available data were used, for ITOP the transit flight data were parsed out, and for the rest of

184   the campaigns only data within the regional boundaries we study (black frames in Figure 3)

185   were used. These boundaries were chosen in accordance with the surface observations.

186   The campaign-average profile was compared against the monthly mean model output, a not

187   uncommon practice in model-aircraft comparison studies (e.g. Bauer et al., 2007; Emmons et

188   al., 2000; Shindell et al., 2003). The simulations were sub-sampled by taking into consideration

189   the geographical variability of the flights, but not the sub-monthly temporal variability, to yield

190   a mean corresponding profile. The one standard deviation variability of the campaign data per

191   model level was calculated for the measurements and model simulations, which represents the

192   spatial variability of the concentrations during the whole field campaign for the measurements,

193   and the spatial variability of the monthly mean modeled concentrations for the model. The

194   duration of the field campaigns ranged from 7 to 17 days. In the Results section we picked 4

195   representative campaigns that display systematic behavior, one for each region (Figure 7). The

196   rest of the campaigns can be found in the appendix (Figure A2, A3).

197   **3. Results and discussion**

198   In terms of mean surface concentrations (measured and modeled) in the Western Hemisphere

199   sulfate concentrations are higher than nitrate concentrations. That is not the case in the

Atmospheric
Chemistry
and Physics
Discussions

Open Access

200   Eastern Hemisphere, since over western Europe sulfate and nitrate aerosols are comparable in

201   mass (Figure 2), consistent with *Schaap et al.* [2004]. At the whole atmospheric column (not

202   shown here), sulfate peaks over east EU and northern Africa due to in-cloud production and

203   transport, while the nitrate column distribution corresponds to the surface distribution, with

204   maxima over the continental hot spots, driven by urban pollution and biomass burning.

205   **3.1 Surface climatology**

206   Surface data show high concentrations of nitrate and sulfate in the industrialized EUSA and EU

207   and lower concentrations in WUSA, with some urban hot spots (Figures 1 and 2). We compared

208   the model skill, with respect to measurements, under the three different aerosol configurations

209   in Figure 4 for nitrate (left) and sulfate (right). The regional clusters observed reflect the fact

210   that performance in terms of R and NMB is controlled by region rather than aerosol scheme.

211   For sulfate, the simulation with no microphysics (OMA, blue) is always biased lower (by 1-4%)

212   compared to the other two simulations (MATRIX, red and green), a result of having sulfate

213   aerosols spread over the entire size distribution, leading to longer lifetime of sulfate mass in

214   MATRIX. As an indication, the mean lifetime of sulfate in 2005 was 4.2 days in the two MATRIX

215   simulations, against 3.2 days in the OMA simulation. We observe a systematic underestimation

216   of ammonium, nitrate and sulfate in EUSA and EU (35% for nitrate, 30% for ammonium, 20% for

217   sulfate). Despite the negative bias, the three aerosol types correlate well with measurements in

218   these regions (R>0.5). This high correlation is due to the fact the simulations successfully

219   capture the aerosol seasonal cycle (discussed in the next section). In the WUSA, the simulations

220   overestimate sulfate by 12%, and underestimated nitrate by 80%, while there is no correlation

221   between the model and observations for nitrate. The different behavior across regions reflects

Atmospheric
Chemistry
and Physics
Discussions

Open Access

222   the fact that the WUSA is driven by agricultural emissions while in the EUSA industrial and

223   residential emissions dominate. The ability of the model to capture the seasonality (discussed

224   in the next section) is important for model skill and is discussed in the next section.

225   **3.2 Surface seasonality**

226   Figure 5 shows that in the EU there is little variation in the SO_2 seasonality between the three

227   simulations, which is emission-level driven. The modeled surface concentration overestimates

228   measurements by about 0.5 μgS m^{-3}, with an amplified seasonal cycle. Past studies (Dentener et

229   al., 2006; Vestreng et al., 2007) have raised concerns regarding the accuracy of SO_2 emission

230   inventories, which might be part of the explanation of the SO_2 overestimation. Additionally,

231   wintertime chemistry slowdown due to reduced photochemistry increases the SO_2 lifetime,

232   resulting in reduced sulfate formation rates, contributing to the underestimation of sulfate

233   concentration which can be as high as a factor of 2 during winter months. For sulfate, the

234   difference between the simulations is dominated by the aerosol scheme, with the summertime

235   peak being more pronounced in the MATRIX simulations than in the OMA one. As explained in

236   the previous section, MATRIX simulates higher concentrations due to the existence of smaller

237   particles with longer lifetimes compared to OMA. Surface NH_3 (Figure 5) is overestimated in all

238   three simulations, which might be due to incorrect NH_x partitioning calculated by EQSAM and

239   ISORROPIA II, a hypothesis that is supported by the underestimate of ammonium. Contrary to

240   SO_2 and NH_3, nitric acid is underestimated by the simulations by a factor of 3. This contributes

241   to the underestimation of nitrate in all simulations**.** The simulated seasonality of nitrate

242   matches that of the measurements, peaking during winter and reaching a minimum during

Atmospheric
Chemistry
and Physics
Discussions

243 summer. *Konovalov et al.* [2008] identified a slight underestimation of NO_x in emission

244 inventories in southern Europe, which would contribute to underestimations of XNO_3.

245 IMPROVE has extensive sulfate and nitrate surface data to compare against the model

246 simulations. EMEP provides additional HNO_3 data from 9 stations, predominantly around the

247 Great Lakes, which is not enough for a proper regional analysis. Unfortunately, ammonium and

248 gas phase aerosol precursors are not routinely measured via the IMPROVE network. In the

249 eastern USA (Figure 6) the model simulations exhibit peak sulfate concentrations during

250 summer, with the MATRIX simulations having a stronger seasonality than OMA, which better

251 matches observations. For nitrate, all simulations systematically underestimate measurements

252 during most of the year (by about 0.2 μg m^{-3}), except during winter, where MATRIX slightly

253 overestimates them (less then 0.1 μg m^{-3}). The HNO_3 underestimation by the model, as evident

254 by the limited measurements we obtained in EUSA (Figure A1), contributes to the nitrate

255 underestimation.

256 In WUSA the simulated sulfate and nitrate seasonality (Figure 6 left panels) is flat compared to

257 the measurements. For sulfate, the measured range is 0.7 μg m^{-3}, while in the MATRIX

258 simulations the range is 0.25 μg m^{-3} and OMA-EQSAM is 0.15 μg m^{-3}. All simulations

259 underestimate measurements during summer and overestimate them during winter. The

260 measured maximum sulfate concentrations are around summer. This feature is captured by

261 OMA-EQSAM, but the MATRIX simulations calculate spring and fall peaks instead. For nitrate,

262 the measurements peak in early winter, a feature that is not captured by the simulations, as

263 modeled nitrate peaks in winter. During the winter OMA-EQSAM and MATRIX EQSAM are

264 similar, probably due to the common thermodynamical scheme, while MATRIX-ISORROPIA II is

Atmospheric
Chemistry
and Physics
Discussions

265   higher by 0.05 μg m^{-3}. Modeled nitrate is underestimated compared to measurements

266   throughout the year: in the MATRIX simulations it is underestimated by about 0.45 μg m^{-3} (80%

267   of the measured value), and in OMA-ISORROPIA it is underestimated by about 0.4 μg m^{-3}.

268   **3.3 Vertical Profiles**

269   The simulated mean vertical profiles of sulfate, ammonium, nitric acid (when available), and

270   nitrate are evaluated against the mean measured profiles in Figure 7. The measured and

271   modeled standard deviations (gray shading and dashed lines, respectively), along with the

272   number of days each layer was sampled (black squares), are shown as well. Generally, aerosol

273   concentrations decrease with altitude as they peak near emission sources at the surface. Some

274   of the data used in this study were affected by intense fire plumes (Fisher et al., 2010; Jacob et

275   al., 2010), as can be seen in the ATCPAC (ARC) and ARCTAS spring and summer (ARC) panels

276   (Figure 7 and A2). Fires act as a source of NO_x, NH_3 and SO_2, increasing the concentration of

277   sulfate, ammonium and nitrate in the measurements. Fire emissions are included in our

278   simulations, yet these emissions could be underestimated, as *Ichoku and Ellison* [2014]

279   indicated is the case in many bottom-up emission inventories such as GFED3 (used here), and

280   are also a function of properly resolving the transport. Even if all these factors are accurate in

281   the model, the monthly mean output we use would dilute the signal of a fire event as observed

282   in a flight profile.

283   Modeled sulfate concentrations are underestimated compared to the measurements (first

284   column in Figure 7 and Figures A2 and A3). The MATRIX simulations that include aerosol

285   microphysics show higher concentrations compared to the bulk scheme. During INTEX-A (EUSA)

Atmospheric
Chemistry
and Physics
Discussions

286   the MATRIX simulations produced in the boundary layer around 1 μg m^{-3} higher sulfate

287   concentrations compared to OMA. The thermodynamic scheme (EQSAM or ISORROPIA II)

288   makes a minor difference for sulfate, stemming from the simulations' climate feedbacks, with

289   the green and red lines overlaying each other. All these results are consistent with the ones

290   presented earlier for the surface.

291   In remote environments like the Florida Keys (CRISTAL-FACE, Figure A3), Azores (ITOP-UK,

292   Figure A3) and the Arctic (ARCTAS spring and summer, Figure 7 and A2), ammonium and nitrate

293   concentrations are generally very low, and the models are able to reproduce the aerosol

294   concentrations. However, in campaigns over land such as: EUCAARI EU, EUSA: INTEX-A, NEAQS,

295   DISCOVER-MD, CALNEX WUSA, TexAQS, and Mexico: MILAGRO-MIRAGE, INTEX-B, there is

296   consistent underestimation of both ammonium and nitrate, especially in the boundary layer

297   (Figures 7, A2 and A3). The sensitivity runs we performed, presented later, explore whether this

298   is due to precursor levels or to the thermodynamic parameterization used.

299   From the nitric acid profiles (third column in Figure 7 and Figure A2), it is evident that the

300   model strongly overestimates the measurements in the middle and upper troposphere. This

301   had been noted before by *Shindell et al.* [2006], who attributed this model overestimation to

302   enhanced stratosphere-troposphere exchange, which brings HNO$_3$-rich air masses from the

303   lower stratosphere to the upper troposphere. On top of that, the modeled nitric acid shows

304   distinct OMA and MATRIX profiles, which diverge with increasing height, with differences that

305   can become as high as 0.3 ppbv. Though there is not much dust at these altitudes, the inclusion

306   of heterogeneous reactions on dust surfaces in OMA is the main difference in the gas phase

307 chemistry of OMA and MATRIX schemes. The coarse mode nitrate mass formed by those

308 heterogeneous reactions almost fully accounts for the difference in HNO_3 between the two

309 schemes. We exclude the nitrate that forms on dust (coarse nitrate) from the nitrate profiles,

310 since neither they are in the PM_1 aerosol measurements, nor they are calculated in the MATRIX

311 simulations.

312 The overestimation of nitric acid does not result in overestimation of nitrate, which is also

313 affected by the availability of both sulfate and ammonia, on top of environmental factors like

314 relative humidity and temperature. Even though nitrate concentrations are low in many

315 locations (below 2 μg m^{-3}), the simulations underestimates it to be below 0.1 μg m^{-3} in EUSA

316 (INTEX-A in Figure 7, NEAQS, DISCOVER-MD, and TexAQS in Figure A2), WUSA (CALNEX in Figure

317 7), arctic (ARCPAC in Figure A2), Central America (INTEX-B in Figure A2, MILAGRO-MIRAGE, and

318 CRISTAL-FACE in Figure A3), consistent with the spring-summer surface underestimation.

319 Another key point is that there is little difference in the nitrate concentrations simulated by the

320 different aerosol configurations. Differences between the simulations are evident only in the

321 boundary layer in EUCAARI (EU, Figure 7), ~0.8 μg m^{-3}, and ACE-ASIA (Japan, Figure A3), ~0.3 μg

322 m^{-3}. In these locations, the difference is not evident on a thermodynamic scheme basis, but

323 rather on a microphysical scheme, with MATRIX-EQSAM and MATRIX-ISORROPIA grouped

324 against OMA-EQSAM. The difference in concentration between the simulations is also evident

325 in the ammonium profiles of these campaigns. In EUCAARI, nitrate and ammonium have higher

326 concentrations in the OMA-EQSAM simulation, while sulfate is consistently larger in the

327 MATRIX ones. In ACE-ASIA however, both sulfate and ammonium concentrations are higher

328 with OMA-EQSAM, yet nitrate concentrations are higher in the MATRIX simulations. It is

Atmospheric
Chemistry
and Physics
Discussions

Open Access

EGU

329   evident from these profiles that the simulations with lower sulfate concentrations are also the

330   simulations with higher nitrate concentrations. The role of thermodynamics to the NH_3/NH_4^+

331   partitioning at different NH_3 levels will be discussed in the next section.

332   **3.4 Sensitivity runs**

333   In order to study the interplay between precursor concentrations and thermodynamics we

334   perturbed the ammonia emissions from agriculture. For these runs, presented in Figure 8, we

335   use the MATRIX-ISORROPIA scheme with standard NH_3 emission (green line), double

336   agricultural NH_3 emissions (purple line) and five times agricultural NH_3 emissions (brown line).

337   At the surface, as NH_3 emissions are increased, the ammonium and nitrate underestimation by

338   the model disappears (Figure 8). However, a comparison with the limited available surface NH_3

339   measurements reveals that even with the standard NH_3 emissions the model overestimates

340   NH_3 concentrations. This is also evident in TexAQS and CALNEX (WUSA) NH_3 profiles (Figure A4).

341   Similarly, in the vertical, with increasing NH_3 emissions the nitric acid model overestimation

342   decreases (Figure A5), as more NH_3 becomes available to react with nitric acid and partition it

343   to the aerosol phase. These results indicate that the NH_3/NH_4^+ partitioning is not accurately

344   calculated by the model, and that this strongly affects the nitric acid/nitrate partitioning.

345   Further evidence to support our conclusion lies in Figure 9 that presents the modeled and

346   measured partitioning ratios (NH_3 over total NH_x, and HNO_3 over total XNO_3). For NH_x all three

347   simulations are grouped together, while for XNO_3 a distinct difference between the

348   thermodynamic schemes is revealed: MATRIX-EQSAM overestimate the partitioning ratio

349   during the summer, and MATRIX-ISORROPIA II is closer to measurements. From the surface

Atmospheric
Chemistry
and Physics
Discussions

350   seasonality of the individual species (Figure 5) it is clear that the divergence in the ratio is

351   driven mainly by nitrate concentrations, as HNO_3 concentrations are the same for MATRIX-

352   EQSAM and MATRIX-ISORROPIA II (red and green curves overlaying each other). The difference

353   between these two simulations in terms of nitrate concentrations are of the order of 0.05 μg N

354   m^{-3} and are most distinct during summer (Figure 5). Similarly, the difference between the

355   simulations for XNO_3 is greater during summer. Thermodynamically, other than precursor

356   levels, the difference in behavior in summer and the rest of the year is also controlled by

357   temperature and RH.

358   **Conclusions**

359   In this work we used a collection of surface measurements and flight campaigns over the USA

360   and Europe from 2000-2010 to study the regional and vertical distribution of secondary

361   inorganic aerosols and their precursors under different aerosol configurations of the GISS

362   ModelE2. In the USA sulfate aerosol dominate the near surface SIA composition, but over EU

363   the nitrate aerosol contribution is comparable in mass.

364   We compare the behavior of SIA concentrations in high (EUSA, EU) and low (WUSA) aerosol

365   precursor source regions, as the relative contribution of different sectors generates different

366   chemical regimes. We observe a systematic underestimation of near surface concentrations in

367   the EUSA and EU compared to the surface network measurements: 35% for nitrate, 30% for

368   ammonium, 20% for sulfate. However, despite the negative bias, all three simulations have high

369   correlation coefficients (R>0.5) when compared against surface data. In the WUSA the results

370   for sulfate and nitrate are different in sign, sulfate is biased high (12%) with R=0.43, while

Atmospheric
Chemistry
and Physics
Discussions

371   nitrate is biased low (80%) with no correlation between the simulations and the measurements

372   (R<0.1). The correlation is also driven by the difficulty of the model to capture the annual cycle

373   of the species.

374   Microphysics has improved the sulfate simulation, as the MATRIX scheme yields consistently,

375   both at the surface and in the vertical, higher sulfate concentrations, due to smaller particles

376   having longer lifetimes compared to OMA, the bulk scheme (4.2 days against 3.2 days). For

377   ammonium nitrate simulations there is an additional level of complexity in the form of accurate

378   thermodynamics, which is sensitive both to the precursors and to environmental parameters

379   such as temperature and humidity. Since we have performed nudged simulations, they do not

380   show big differences in temperature and RH, so the differences between the simulations are

381   expected to be dominated by the thermodynamical scheme and not the underlying

382   meteorological parameters. In terms of precursors, NH_3 is slightly overestimated, as indicated

383   by surface measurements over EU in Figure 5 and TexAQS and CALNEX campaigns in Figure A3.

384   HNO_3 is underestimated at the surface but overestimated at higher levels. The overestimation

385   is attributed to too strong stratosphere-troposphere exchange, yet including heterogeneous

386   reactions on dust surfaces decreases the overestimation. Overall, aerosol mass is consistently

387   underestimated both at surface and in the boundary layer.

388   In our sensitivity runs, increasing NH_3 emissions results in NH_3 overestimation, however it

389   improves our simulated HNO_3 profiles. When more NH_3 is available it reacts with HNO_3 to form

390   ammonium nitrate, resolving underestimations in the aerosol phase. Hence, the partitioning of

391   NH_x which strongly affects the partitioning of XNO_3 is not accurately simulated in the model.

Atmospheric
Chemistry
and Physics
Discussions

Open Access

EGU

392   *Aan de Brugh et al.* [2012] identified an overestimation of gas phase precursors during daytime

393   (equivalent to summer) and overestimation of aerosol phase species during nighttime

394   (equivalent to winter), and found it to be related to the time scale of vertical mixing against the

395   timescale of thermodynamic equilibrium. This relationship was not analyzed here, since it

396   requires high temporal resolution model output.

397   An examination of aerosol pH (not presented here) indicated a pH rage from 1 to 2 over EU.

398   This range was recently identified by *Weber et al.* [2016] as a buffering pH zone where

399   partitioning of ammonium nitrate between the gas and aerosol phases is sensitive. Thus, ions

400   which affect pH might play an important role in nitrate formation. Hence, taking into

401   consideration crustal and sea salt ions could affect our thermodynamics and partitioning in

402   regions where these ions are abundant, as *Karydis et al.* [2016] demonstrated. However, these

403   are currently tracked as bulk dust and sea salt aerosols in the model. In addition to tracking Na^+,

404   Cl^-, etc. separately, we would need to consider the different time scales of the thermodynamics

405   associated with aerosol size distribution. In the future, we plan to investigate the influence of

406   pH on the results in more detail.

407   In this paper we have demonstrated the importance of size resolved sulfate chemistry.

408   However, currently we treat nitrate as bulk, as it is computationally expensive to add 15 nitrate

409   tracers. Perhaps underestimation of nitrate is not only a matter of thermodynamics but

410   microphysics as well, and that properly resolving the size distribution, and considering the

411   chemistry that depends on that would improve our simulations.

Atmospheric
Chemistry
and Physics
Discussions

Open Access

EGU

422   **References**

423

424   Aan de Brugh, J. M. J., Henzing, J. S., Schaap, M., Morgan, W. T., van Heerwaarden, C. C.,
425   Weijers, E. P., Coe, H. and Krol, M. C.: Modelling the partitioning of ammonium nitrate in the
426   convective boundary layer, Atmos. Chem. Phys., 12(6), 3005–3023, doi:10.5194/acp-12-3005-
427   2012, 2012.

428   Adams, P. J., Seinfeld, J. H. and Koch, D. M.: Global concentrations of tropospheric sulfate,
429   nitrate, and ammonium aerosol simulated in a general circulation model, J. Geophys. Res., 104,
430   13791–13823, 1999.

431   Allan, J. D., Jimenez, J. L., Williams, P. I., Alfarra, M. R., Bower, K. N., Jayne, J. T., Coe, H. and
432   Worsnop, D. R.: Quantitative sampling using an Aerodyne aerosol mass spectrometer: 1.
433   Techniques of data interpretation and error analysis, J. Geophys. Res., 108,
434   doi:10.1029/2003JD001608, 2003.

435   Anderson, D. C., Loughner, C. P., Diskin, G., Weinheimer, A., Canty, T. P., Salawitch, R. J.,
436   Worden, H. M., Fried, A., Mikoviny, T., Wisthaler, A. and Dickerson, R. R.: Measured and
437   modeled CO and NOy in DISCOVER-AQ: An evaluation of emissions and chemistry over the
438   eastern US, Atmos. Environ., 96, 78–87, doi:10.1016/j.atmosenv.2014.07.004, 2014.

439   Bauer, S. E. and Koch, D.: Impact of heterogeneous sulfate formation at mineral dust surfaces
440   on aerosol loads and radiative forcing in the Goddard Institute for Space Studies general
441   circulation model, J. Geophys. Res. D Atmos., 110, 91–105, doi:10.1029/2005JD005870, 2005.

442   Bauer, S. E. and Menon, S.: Aerosol direct , indirect , semidirect , and surface albedo effects
443   from sector contributions based on the IPCC AR5 emissions for preindustrial and present-day
444   conditions, , 117, 1–15, doi:10.1029/2011JD016816, 2012.

445   Bauer, S. E., Balkanaki, Y., Schulz, M. and Hauglustaine, D. A.: Global modeling of
446   heterogeneous chemistry on mineral aerosol surfaces: Influence on tropospheric ozone
447   chemistry and comparison to observations, J. Geophys. Res., 109, 1–17,

448   doi:10.1029/2003JD003868, 2004.

449   Bauer, S. E., Koch, D., Unger, N., Metzger, S. M., Shindell, D. T. and Streets, D. G.: Nitrate
450   aerosols today and in 2030: a global simulation including aerosols and tropospheric ozone,
451   Atmos. Chem. Phys., 7, 5043–5059, doi:10.5194/acp-7-5043-2007, 2007.

452   Bauer, S. E., Wright, D., Koch, D., Lewis, E. R., McGraw, R., Chang, L.-S., Schwartz, S. E. and
453   Ruedy, R.: MATRIX (Multiconfiguration Aerosol TRacker of mIXing state): an aerosol
454   microphysical module for global atmospheric models, Atmos. Chem. Phys., 8, 6003–6035,
455   doi:10.5194/acpd-8-9931-2008, 2008.

456   Benduhn, F., Mann, G. W., Pringle, K. J., Topping, D. O., Mcfiggans, G. and Carslaw, K. S.: Size-
457   resolved simulations of the aerosol inorganic composition with the new hybrid dissolution
458   solver HyDiS-1 . 0 – Description , evaluation and first global modelling results, , (February), 1–
459   54, doi:10.5194/gmd-2015-264, 2016.

460   Conant, W. C., Vanreken, T. M., Rissman, T. A., Varutbangkul, V., Jonsson, H. H., Nenes, A.,
461   Jimenez, J. L., Delia, A. E., Bahreini, R., Roberts, G. C. and Flagan, R. C.: Aerosol--cloud drop
462   concentration closure in warm cumulus, , 109, 1–12, doi:10.1029/2003JD004324, 2004.

463   van Damme, M., Erisman, J. W., Clarisse, L., Dammers, E., Whitburn, S., Clerbaux, C., Dolman, A.
464   J. and Coheur, P.: Worldwide spatiotemporal atmospheric ammonia (NH3) columns variability
465   revealed by satellite, , 1–9, doi:10.1002/2015GL065496.We, 2015.

466   DeCarlo, P. F., Dunlea, E. J., Kimmel, J. R., Aiken, A. C., Sueper, D., Crounse, J., Wennberg, P. O.,
467   Emmons, L., Shinozuka, Y., Clarke, A., Zhou, J., Tomlinson, J., Collins, D. R., Knapp, D.,
468   Weinheimer, A. J., Montzka, D. D., Campos, T. and Jimenez, J. L.: Fast airborne aerosol size and
469   chemistry measurements above Mexico City and Central Mexico during the MILAGRO
470   campaign, Atmos. Chem. Phys., 8(14), 4027–4048, doi:10.5194/acp-8-4027-2008, 2008.

471   Dentener, F., Drevet, J., Lamarque, J. F., Bey, I., Eickhout, B., Fiore, a. M., Hauglustaine, D.,
472   Horowitz, L. W., Krol, M., Kulshrestha, U. C., Lawrence, M., Galy-Lacaux, C., Rast, S., Shindell, D.,
473   Stevenson, D., Van Noije, T., Atherton, C., Bell, N., Bergman, D., Butler, T., Cofala, J., Collins, B.,
474   Doherty, R., Ellingsen, K., Galloway, J., Gauss, M., Montanaro, V., Müller, J. F., Pitari, G.,
475   Rodriguez, J., Sanderson, M., Solmon, F., Strahan, S., Schultz, M., Sudo, K., Szopa, S. and Wild,
476   O.: Nitrogen and sulfur deposition on regional and global scales: A multimodel evaluation,
477   Global Biogeochem. Cycles, 20(4), n/a–n/a, doi:10.1029/2005GB002672, 2006.

478   EMEP: EMEP Manual for Sampling and Analysis, EMEP, available at: http://www.nilu.no/
479   projects/ccc/manual/index.html (last access: 30 October 2015), 2014. 29714, 29723

480   Emmons, L. K., Hauglustaine, D. a., Müller, J.-F., Carroll, M. A., Brasseur, G. P., Brunner, D.,

Atmospheric
Chemistry
and Physics
Discussions

Open Access

EGU

481 Staehelin, J., Thouret, V. and Marenco, A.: Data composites of airborne observations of
482 tropospheric ozone and its precursors, J. Geophys. Res., 105, 20497,
483 doi:10.1029/2000JD900232, 2000.

484 Fehsenfeld, F. C., Ancellet, G., Bates, T. S., Goldstein, a. H., Hardesty, R. M., Honrath, R., Law, K.
485 S., Lewis, a. C., Leaitch, R., McKeen, S., Meagher, J., Parrish, D. D., Pszenny, a. a P., Russell, P.
486 B., Schlager, H., Seinfeld, J., Talbot, R. and Zbinden, R.: International Consortium for
487 Atmospheric Research on Transport and Transformation (ICARTT): North America to Europe -
488 Overview of the 2004 summer field study, J. Geophys. Res. Atmos., 111,
489 doi:10.1029/2006JD007829, 2006.

490 Fisher, J. a., Jacob, D. J., Purdy, M. T., Kopacz, M., Le Sager, P., Carouge, C., Holmes, C. D.,
491 Yantosca, R. M., Batchelor, R. L., Strong, K., Diskin, G. S., Fuelberg, H. E., Holloway, J. S., Hyer, E.
492 J., McMillan, W. W., Warner, J., Streets, D. G., Zhang, Q., Wang, Y. and Wu, S.: Source
493 attribution and interannual variability of Arctic pollution in spring constrained by aircraft
494 (ARCTAS, ARCPAC) and satellite (AIRS) observations of carbon monoxide, Atmos. Chem. Phys.,
495 10, 977–996, doi:10.5194/acpd-9-19035-2009, 2010.

496 Fountoukis, C. and Nenes, a: ISORROPIA II: a computationally efficient thermodynamic
497 equilibrium model for K+–Ca2+–Mg2+–NH4+–Na+–SO42−–NO3−–Cl−–H2O aerosols, Atmos.
498 Chem. Phys., 7, 4639–4659, doi:10.5194/acp-7-4639-2007, 2007.

499 Hand, J. L., Copeland, S. a., Day, D. E., Dillner, A. M., Indresand, H., Malm, W. C., McDade, C. E.,
500 Moore, C. T., Pitchford, M. L., Schichtel, B. a. and Watson, J. G.: Spatial and Seasonal Patterns
501 and Temporal Variability of Haze and its Constituents in the United States Report V., 2011.

502 Hand, J. L., Schichtel, B. A., Pitchford, M., Malm, W. C. and Frank, N. H.: Seasonal composition of
503 remote and urban fine particulate matter in the United States, J. Geophys. Res., 117(D5),
504 D05209, doi:10.1029/2011JD017122, 2012.

505 Hauglustaine, D. a., Balkanski, Y. and Schulz, M.: A global model simulation of present and
506 future nitrate aerosols and their direct radiative forcing of climate, Atmos. Chem. Phys., 14(20),
507 11031–11063, doi:10.5194/acp-14-11031-2014, 2014.

508 Haywood, J. and Boucher, O.: Estimates of the Direct and Indirect Radiative Forcing Due to
509 Tropospheric Aerosols: A Review, Rev. Geophys., 38(4), 513–543, 2000.

510 Heald, C. L., Jacob, D. J., Park, R. J., Russell, L. M., Huebert, B. J., Seinfeld, J. H., Liao, H. and
511 Weber, R. J.: A large organic aerosol source in the free troposphere missing from current
512 models, Geophys. Res. Lett., 32(18), 1–4, doi:10.1029/2005GL023831, 2005.

513 Heald, C. L., Coe, H., Jimenez, J. L., Weber, R. J., Bahreini, R., Middlebrook, a. M., Russell, L. M.,

Atmospheric
Chemistry
and Physics
Discussions

Open Access

EGU

514   Jolleys, M., Fu, T.-M., Allan, J. D., Bower, K. N., Capes, G., Crosier, J., Morgan, W. T., Robinson,
515   N. H., Williams, P. I., Cubison, M. J., DeCarlo, P. F. and Dunlea, E. J.: Exploring the vertical profile
516   of atmospheric organic aerosol: comparing 17 aircraft field campaigns with a global model,
517   Atmos. Chem. Phys., 11(24), 12673–12696, doi:10.5194/acp-11-12673-2011, 2011.

518   Hodas, N., Sullivan, A. P., Skog, K., Keutsch, F. N., Collett, J. L., Decesari, S., Facchini, M. C.,
519   Carlton, A. G., Laaksonen, A. and Turpin, B. J.: Aerosol liquid water driven by anthropogenic
520   nitrate: implications for lifetimes of water-soluble organic gases and potential for secondary
521   organic aerosol formation., Environ. Sci. Technol., 48(19), 11127–36, doi:10.1021/es5025096,
522   2014.

523   Huebert, B. J.: An overview of ACE-Asia: Strategies for quantifying the relationships between
524   Asian aerosols and their climatic impacts, J. Geophys. Res., 108(D23), 8633,
525   doi:10.1029/2003JD003550, 2003.

526   Ichoku, C. and Ellison, L.: Global top-down smoke-aerosol emissions estimation using satellite
527   fire radiative power measurements, Atmos. Chem. Phys., 14, 6643–6667, doi:10.5194/acp-14-
528   6643-2014, 2014.

529   Jacob, D. J., Crawford, J. H., Maring, H., Clarke, a. D., Dibb, J. E., Emmons, L. K., Ferrare, R. a.,
530   Hostetler, C. a., Russell, P. B., Singh, H. B., Thompson, a. M., Shaw, G. E., McCauley, E.,
531   Pederson, J. R. and Fisher, J. a.: The arctic research of the composition of the troposphere from
532   aircraft and satellites (ARCTAS) mission: Design, execution, and first results, Atmos. Chem.
533   Phys., 10, 5191–5212, doi:10.5194/acp-10-5191-2010, 2010.

534   Jimenez, J. L., Jayne, J. T., Shi, Q., Kolb, C. E., Worsnop, D. R., Yourshaw, I., Seinfeld, J. H., Flagan,
535   R. C., Zhang, X., Smith, K. A., Morris, J. W. and Davidovits, P.: Ambient aerosol sampling using
536   the Aerodyne Aerosol Mass Spectrometer, J. Geophys. Res., 108(D7), 8425,
537   doi:10.1029/2001jd001213, 2003.

538   Kalnay, E., Kanamitsu, M., Kistler, R., Collins, W., Deaven, D., Gandin, L., Iredell, M., Saha, S.,
539   White, G., Woollen, J., Zhu, Y., Chelliah, M., Ebisuzaki, W., Higgins, W., Janowiak, J., Mo, K. C.,
540   Ropelewski, C., Wang, J., Leetmaa, A., Reynolds, R., Jenne, R. and Joseph, D.: The NCEP/NCAR
541   40-Year Reanalysis Project, Bull. Am. Meteorol. Soc., 77(2), 437–471, 1996.

542   Karydis, V. a., Tsimpidi, a. P., Pozzer, A., Astitha, M. and Lelieveld, J.: Effects of mineral dust on
543   global atmospheric nitrate concentrations, Atmos. Chem. Phys., 16, 1491–1509,
544   doi:10.5194/acpd-15-11525-2015, 2016.

545   Koch, D., D. Jacob, I. Tegen, D. Rind, and M. Chin, 1999: Tropospheric sulfur simulation and
546   sulfate direct radiative forcing in the Goddard Institute for Space Studies general circulation

547   model. *J. Geophys. Res.*, **104**, 23799-23822, doi:10.1029/1999JD900248.

548   Koch, D., Schmidt, G. a. and Field, C. V.: Sulfur, sea salt, and radionuclide aerosols in GISS
549   ModelE, J. Geophys. Res. Atmos., 111(December 2005), doi:10.1029/2004JD005550, 2006.

550   Konovalov, I. B., Beekmann, M., Burrows, J. P. and Richter, a.: Satellite measurement based
551   estimates of decadal changes in European nitrogen oxides emissions, Atmos. Chem. Phys.
552   Discuss., 8(1), 2013–2059, doi:10.5194/acpd-8-2013-2008, 2008.

553   Lamarque, J.-F., Bond, T. C., Eyring, V., Granier, C., Heil, A., Klimont, Z., Lee, D., Liousse, C.,
554   Mieville, A., Owen, B., Schultz, M. G., Shindell, D., Smith, S. J., Stehfest, E., Van Aardenne, J.,
555   Cooper, O. R., Kainuma, M., Mahowald, N., McConnell, J. R., Naik, V., Riahi, K. and van Vuuren,
556   D. P.: Historical (1850–2000) gridded anthropogenic and biomass burning emissions of reactive
557   gases and aerosols: methodology and application, Atmos. Chem. Phys., 10, 7017–7039,
558   doi:10.5194/acp-10-7017-2010, 2010.

559   Leaitch, W. R., Macdonald, a. M., Anlauf, K. G., Liu, P. S. K., Toom-Sauntry, D., Li, S.-M., Liggio,
560   J., Hayden, K., Wasey, M. a., Russell, L. M., Takahama, S., Liu, S., van Donkelaar, A., Duck, T.,
561   Martin, R. V., Zhang, Q., Sun, Y., McKendry, I., Shantz, N. C. and Cubison, M.: Evidence for Asian
562   dust effects from aerosol plume measurements during INTEX-B 2006 near Whistler, BC, Atmos.
563   Chem. Phys. Discuss., 8, 18531–18589, doi:10.5194/acpd-8-18531-2008, 2009.

564   Lohmann, U. and Feichter, J.: Global indirect aerosol effects : a review, Atmos. Chem. Phys., 5,
565   715–737, 2005.

566   Malm, W. C., Sisler, J. F., Huffman, D., Eldred, R. A. and Cahill, T. A.: SPATIAL AND SEASONAL
567   TRENDS IN PARTICLE CONCENTRATION AND OPTICAL EXTINCTION IN THE UNITED-STATES, J.
568   Geophys. Res., 99, 1347–1370, 1994.

569   Malm, W. C., Schichtel, B. A., Pitchford, M. L., Ashbaugh, L. L. and Eldred, R. A.: Spatial and
570   monthly trends in speciated fine particle concentration in the United States, J. Geophys. Res.,
571   109, doi:10.1029/2003JD003739, 2004.

572   Metzger, S., Dentener, F., Krol, M., Jeuken, A. and Lelieveld, J.: Gas/aerosol partitioning 2.
573   Global modeling results, J. Geophys. Res. D Atmos., 107(August), 1–23, 2002a.

574   Metzger, S., Dentener, F., Pandis, S. and Lelieveld, J.: Gas/aerosol partitioning: 1. A
575   computationally efficient model, J. Geophys. Res. Atmos., 107(August),
576   doi:10.1029/2001JD001102, 2002b.

577   Miller, R. L., Cakmur, R. V., Perlwitz, J., Geogdzhayev, I. V., Ginoux, P., Koch, D., Kohfeld, K. E.,
578   Prigent, C., Ruedy, R., Schmidt, G. a. and Tegen, I.: Mineral dust aerosols in the NASA Goddard
579   Institute for Space Sciences ModelE atmospheric general circulation model, J. Geophys. Res.

Atmospheric
Chemistry
and Physics
Discussions

580   Atmos., 111, 1–19, doi:10.1029/2005JD005796, 2006.

581   Morgan, W. T., Allan, J. D., Bower, K. N., Esselborn, M., Harris, B., Henzing, J. S., Highwood, E. J.,
582   Kiendler-Scharr, a., McMeeking, G. R., Mensah, a. a., Northway, M. J., Osborne, S., Williams, P.
583   I., Krejci, R. and Coe, H.: Enhancement of the aerosol direct radiative effect by semi-volatile
584   aerosol components: airborne measurements in North-Western Europe, Atmos. Chem. Phys.,
585   10(17), 8151–8171, doi:10.5194/acp-10-8151-2010, 2010.

586   Park, R. J.: Natural and transboundary pollution influences on sulfate-nitrate-ammonium
587   aerosols in the United States: Implications for policy, J. Geophys. Res., 109(D15), D15204,
588   doi:10.1029/2003JD004473, 2004.

589   Parrish, D. D., Allen, D. T., Bates, T. S., Estes, M., Fehsenfeld, F. C., Feingold, G., Ferrare, R.,
590   Hardesty, R. M., Meagher, J. F., Nielsen-Gammon, J. W., Pierce, R. B., Ryerson, T. B., Seinfeld, J.
591   H. and Williams, E. J.: Overview of the second texas air quality study (TexAQS II) and the Gulf of
592   Mexico atmospheric composition and climate study (GoMACCS), J. Geophys. Res. Atmos., 114,
593   1–28, doi:10.1029/2009JD011842, 2009.

594   Paulot, F., Jacob, D. J., Pinder, R. W., Bash, J. O., Travis, K. and Henze, D. K.: Ammonia emissions
595   in the United States, European Union, and China derived by high-resolution inversion of
596   ammonium wet deposition data: Interpretation with a new agricultural emissions inventory
597   (MASAGE-NH3), J. Geophys. Res. Atmos., 119(7), 4343–4364, doi:10.1002/2013JD021130, 2014.

598   Paulot, F., Ginoux, P., Cooke, W. F., Donner, L. J., Fan, S., Lin, M., Mao, J., Naik, V. and Horowitz,
599   L. W.: Sensitivity of nitrate aerosols to ammonia emissions and to nitrate chemistry:
600   implications for present and future nitrate optical depth, Atmos. Chem. Phys., 15(18), 25739–
601   25788, doi:10.5194/acpd-15-25739-2015, 2016.

602   Potukuchi, S. and Wexler, A. S.: Identifying solid-aqueous-phase transitions in atmospheric
603   aerosols. II. Acidic solutions, Atmos. Environ., 29(22), 3357–3364, doi:10.1016/1352-
604   2310(95)00212-H, 1995a.

605   Potukuchi, S. and Wexler, S. A.: Identifying solid-aqueous-phase transitions in atmospheric
606   aerosols. I. Neutral-acidity solutions, Atmos. Environ., 29(14), 1995b.

607   Pusede, S. E., Duffey, K. C., Shusterman, a. a., Saleh, A., Laughner, J. L., Wooldridge, P. J., Zhang,
608   Q., Parworth, C. L., Kim, H., Capps, S. L., Valin, L. C., Cappa, C. D., Fried, A., Walega, J., Nowak, J.
609   B., Hoff, R. M., Berkoff, T. a., Beyersdorf, a. J., Olson, J., Crawford, J. H. and Cohen, R. C.: On the
610   effectiveness of nitrogen oxide reductions as a control over ammonium nitrate aerosol, Atmos.
611   Chem. Phys., 15(19), 27087–27136, doi:10.5194/acpd-15-27087-2015, 2016.

612   Ravishankara, A. R.: Heterogeneous and Multiphase Chemistry in the Troposphere, Science (80-

Atmospheric
Chemistry
and Physics
Discussions

613   .)., 276(5315), 1058–1065, doi:10.1126/science.276.5315.1058, 1997.

614   Rayner, N. A., Parker, D. E., Horton, E. B., Folland, C. K., Alexander, L. V., Rowell, D. P., Kent, E. C.
615   and Kaplan, A.: Global analyses of sea surface temperature, sea ice, and night marine air
616   temperature since the late nineteenth century, J. Geophys. Res., 108(D14), 4407,
617   doi:10.1029/2002JD002670, 2003.

618   Ryerson, T. B., Andrews, a. E., Angevine, W. M., Bates, T. S., Brock, C. a., Cairns, B., Cohen, R. C.,
619   Cooper, O. R., De Gouw, J. a., Fehsenfeld, F. C., Ferrare, R. a., Fischer, M. L., Flagan, R. C.,
620   Goldstein, a. H., Hair, J. W., Hardesty, R. M., Hostetler, C. a., Jimenez, J. L., Langford, a. O.,
621   McCauley, E., McKeen, S. a., Molina, L. T., Nenes, a., Oltmans, S. J., Parrish, D. D., Pederson, J.
622   R., Pierce, R. B., Prather, K., Quinn, P. K., Seinfeld, J. H., Senff, C. J., Sorooshian, a., Stutz, J.,
623   Surratt, J. D., Trainer, M., Volkamer, R., Williams, E. J. and Wofsy, S. C.: The 2010 California
624   Research at the Nexus of Air Quality and Climate Change (CalNex) field study, J. Geophys. Res.
625   Atmos., 118, 5830–5866, doi:10.1002/jgrd.50331, 2013.

626   Schaap, M., van Loon, M., ten Brink, H. M., Dentener, F. J. and Builtjes, P. J. H.: Secondary
627   inorganic aerosol simulations for Europe with special attention to nitrate, Atmos. Chem. Phys.,
628   4(3), 857–874, doi:10.5194/acp-4-857-2004, 2004.

629   Schmidt, G. a, Kelley, M., Nazarenko, L., Ruedy, R., Russell, G. L., Aleinov, I., Bauer, M., Bauer, S.
630   E., Bhat, M. K., Bleck, R., Canuto, V., Chen, Y., Cheng, Y., Clune, T. L., Genio, A. Del, Fainchtein, R.
631   De, Faluvegi, G., Hansen, J. E., Healy, R. J., Kiang, N. Y., Koch, D., Lacis, A. a, Legrande, A. N.,
632   Lerner, J., Lo, K. K., Matthews, E. E., Menon, S., Miller, R. L., Oinas, V., Oloso, A. O., Perlwitz, J.
633   P., Puma, M. J., Putman, W. M., Rind, D., Romanou, A., Sato, M., Shindell, D. T., Sun, S., Syed, R.
634   A., Tausnev, N., Tsigaridis, K., Unger, N., Voulgarakis, A., Yao, M.-S. and Zhang, J.: Configuration
635   and assessment of the GISS ModelE2 contributions to the CMIP5 archive, J. Adv. Model. Earth
636   Syst., 6, 141–184, doi:10.1002/2013MS000265.Received, 2014.

637   Shindell, D. T., Garenfell, L. J., Rind, D., Grewel, V. and Price, C.: Chemistry-climate interactions
638   in the Goddard Institute for Space Studies general circulation model 1. Tropospheric chemistry
639   model description and evaluation, J. Geophys. Res., 106(D8), 8047–8075, 2001.

640   Shindell, D. T., Faluvegi, G. and Bell, N.: Preindustrial-to-present-day radiative forcing by
641   tropospheric ozone from improved simulations with the GISS chemistry-climate GCM, Atmos.
642   Chem. Phys., 3, 3939–3989, doi:10.5194/acpd-3-3939-2003, 2003.

643   Shindell, D. T., Faluvegi, G., Aguilar, E., Schmidt, G. A., Koch, D. M., Bauer, S. E. and Miller, R. L.:
644   Simulations of preindustrail, present-day, and 2100 conditions in the NASA GISS composition
645   and climate model G-PUCCINI, Atmos. Chem. Phys., 6, 4427–4459, 2006.

Atmospheric
Chemistry
and Physics

Discussions

Open Access

646   Shindell, D. T., Lamarque, J. F., Schulz, M., Flanner, M., Jiao, C., Chin, M., Young, P. J., Lee, Y. H.,

647   Rotstayn, L., Mahowald, N., Milly, G., Faluvegi, G., Balkanski, Y., Collins, W. J., Conley, a. J.,

648   Dalsoren, S., Easter, R., Ghan, S., Horowitz, L., Liu, X., Myhre, G., Nagashima, T., Naik, V.,

649   Rumbold, S. T., Skeie, R., Sudo, K., Szopa, S., Takemura, T., Voulgarakis, a., Yoon, J. H. and Lo, F.:

650   Radiative forcing in the ACCMIP historical and future climate simulations, Atmos. Chem. Phys.,

651   13(6), 2939–2974, doi:10.5194/acp-13-2939-2013, 2013.

652   Singh, H. B., Brune, W. H., Crawford, J. H., Jacob, D. J. and Russell, P. B.: Overview of the

653   summer 2004 Intercontinental Chemical Transport Experiment-North America (INTEX-A), J.

654   Geophys. Res. Atmos., 111(December), doi:10.1029/2006JD007905, 2006.

655   Stocker, T. F., D. Qin, G.-K. Plattner, M. Tignor, S.K. Allen, J. Boschung, A. Nauels, Y. Xia, V. Bex

656   and P.M. Midgley (eds.): IPCC, 2013: Summary for Policymakers. In: Climate Change 2013: The

657   Physical Science Basis. Contribution of Working Group I to the Fifth Assessment Report of the

658   Intergovernmental Panel on Climate Change, Cambridge University Press, Cambridge, United

659   Kingdom and New York, NY, USA., 2013.

660   Tagaris, E., Manomaiphiboon, K., Liao, K. J., Leung, L. R., Woo, J. H., He, S., Amar, P. and Russell,

661   A. G.: Impacts of global climate change and emissions on regional ozone and fine particulate

662   matter concentrations over the United States, J. Geophys. Res. Atmos., 112,

663   doi:10.1029/2006JD008262, 2007.

664   Tørseth, K., Aas, W., Breivik, K., Fjeraa, A. M., Fiebig, M., Hjellbrekke, A. G., Lund Myhre, C.,

665   Solberg, S. and Yttri, K. E.: Introduction to the European Monitoring and Evaluation Programme

666   (EMEP) and observed atmospheric composition change during 1972-2009, Atmos. Chem. Phys.,

667   12(12), 5447–5481, doi:10.5194/acp-12-5447-2012, 2012.

668   Vestreng, V., Myhre, G., Fagerli, H., Reis, S. and Tarrasón, L.: Twenty-five years of continuous

669   sulphur dioxide emission reduction in Europe, Atmos. Chem. Phys., 7(13), 3663–3681,

670   doi:10.5194/acp-7-3663-2007, 2007.

671   van Vuuren, D. P., Edmonds, J., Kainuma, M., Riahi, K., Thomson, A., Hibbard, K., Hurtt, G. C.,

672   Kram, T., Krey, V., Lamarque, J. F., Masui, T., Meinshausen, M., Nakicenovic, N., Smith, S. J. and

673   Rose, S. K.: The representative concentration pathways: An overview, Clim. Change, 109, 5–31,

674   doi:10.1007/s10584-011-0148-z, 2011.

675   Weber, R. J., Orsini, D., Daun, Y., Lee, Y.-N., Klotz, P. J. and Brechtel, F.: A Particle-into-Liquid

676   Collector for Rapid Measurement of Aerosol Bulk Chemical Composition, Aerosol Sci. Technol.,

677   35(February 2015), 718–727, doi:10.1080/02786820152546761, 2001.

678   Weber, R. J., Guo, H., Russell, A. G. and Nenes, A.: High aerosol acidity despite declining

Atmospheric
Chemistry
and Physics
Discussions

Open Access

EGU

679   atmospheric sulfate concentrations over the past 15 years, Nat. Geosci.,

680   doi:10.1038/NGEO2665, 2016.

681   van der Werf, G. R., Randerson, J. T., Giglio, L., Collatz, G. J., Mu, M., Kasibhatla, P. S., Morton,

682   D. C., Defries, R. S., Jin, Y. and van Leeuwen, T. T.: Global fire emissions and the contribution of

683   deforestation, savanna, forest, agricultural, and peat fires (1997-2009), Atmos. Chem. Phys., 10,

684   11707–11735, doi:10.5194/acp-10-11707-2010, 2010.

685   Xu, L. and Penner, J. E.: Global simulations of nitrate and ammonium aerosols and their

686   radiative effects, Atmos. Chem. Phys., 12(20), 9479–9504, doi:10.5194/acp-12-9479-2012,

687   2012.

688   Ziemba, L. D., Thornhill, K. L., Ferrare, R., Barrick, J., Beyersdorf, A. J., Chen, G., Crumeyrolle, S.

689   N., Hair, J., Hostetler, C., Hudgins, C., Obland, M., Rogers, R., Scarino, A. J., Winstead, E. L. and

690   Anderson, B. E.: Airborne observations of aerosol extinction by in situ and remote-sensing

691   techniques: Evaluation of particle hygroscopicity, Geophys. Res. Lett., 40(2), 417–422,

692   doi:10.1029/2012GL054428, 2013.

693

694

695

696

697

698

699

700

701

702

703

704

705

706

707

Atmospheric
Chemistry
and Physics
Discussions

Open Access

708   **Table 1.** Regional boundaries for data division

709

| Region	Boundaries
Arctic (ARC)	55°-90°N, 60°-170°W
Eastern USA (EUSA)	30°-50°N, 60°-95°W
Western USA (WUSA)	30°-50°N, 114°-130°W
European Union (EU)	35°-70°N, 10°W-30°E

710

711
712
713
714
715
716
717
718
719
720
721
722
723
724
725
726
727
728
729
730
731
732
733
734
735
736
737
738
739
740
741

Atmospheric
Chemistry
and Physics
Discussions

742   **Table 2.** Airborne measurements used in this study.
743
744

Campaign (Aircraft)	Region (season, year)	Technique and reference	Regime
ACE-Asia (CIPRAS TWIN OTTER)	Japan (spring, 2001)	AMS (Huebert, 2003)	Polluted
CRYSTAL-FACE (CIPRAS TWIN OTTER)	South Florida (summer, 2002)	AMS (Conant et al., 2004)	Polluted
ITOP (BAE-146)	Azores (summer, 2004)	AMS (Fehsenfeld et al., 2006)	Remote
INTEX-A (DC-8, J-31)	Eastern USA (summer, 2004)	CIMS (HNO_3), PILS (SO_4,NH_4,NO_3) (Singh et al., 2006)	Polluted
NEAQS (NOAA-P3)	Eastern USA (summer, 2004)	CIMS (HNO_3), AMS (SO_4, NH_4, NO_3) (Fehsenfeld et al., 2006)	Polluted
INTEX-B (DC-8)	Western USA (spring, 2006)	CIMS (HNO_3), AMS (SO_4,NH_4,NO_3) (Leaitch et al., 2009)	Polluted
MILAGRO (C120)	Mexico (spring, 2006)	AMS (DeCarlo et al., 2008)	Polluted
TexAQS (NOAA-P3)	Texas (fall, 2006)	CIMS (NH3, HNO_3), AMS (SO_4, NH_4, NO_3) (Parrish et al., 2009)	Polluted
EUCAARI (BAE-146)	NW EU (spring, 2008)	AMS (Morgan et al., 2010)	Polluted
ARCPAC (NOAA-P3	Arctic (spring, 2008)	CIMS (HNO_3), AMS (SO_4, NH_4, NO_3) (Fisher et al., 2010)	Fire
ARCTAS (DC-8, P-3)	Arctic (spring/summer 2008)	CIMS (HNO_3), AMS (SO_4, NH_4, NO_3) (Jacob et al., 2010)	Fire
CALNEX (NOAA P-3)	West coast (summer, 2010)	CIMS (HNO_3, NH_3), AMS (SO_4, NH_4, NO_3) (Ryerson et al., 2013)	Polluted
DISCOVER-MD (P-3B, UC-12)	Maryland (summer, 2011)	TD-LIF (HNO_3) (Anderson et al., 2014), PILS (SO_4, NH_4, NO_3) (Ziemba et al., 2013)	Polluted

745

Atmospheric
Chemistry
and Physics
Discussions
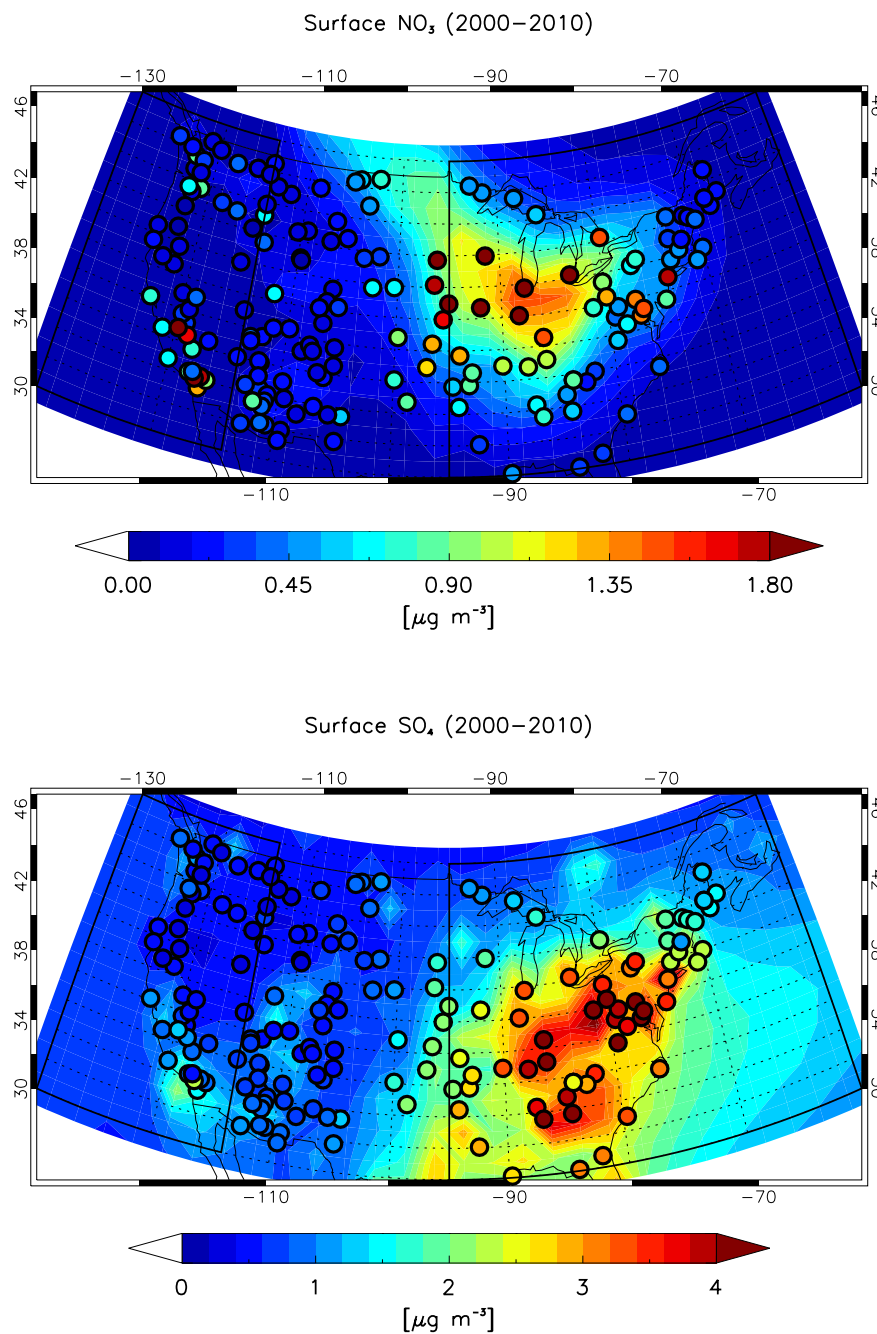
Figure 1. Mean nitrate (upper panel) and sulfate (lower panel) surface concentration (2000-2010) simulated by MATRIX-EQSAM overlaid by measurements from the IMPROVE network. The model data units match the units of the measured data ($\mu g\ m^{-3}$).
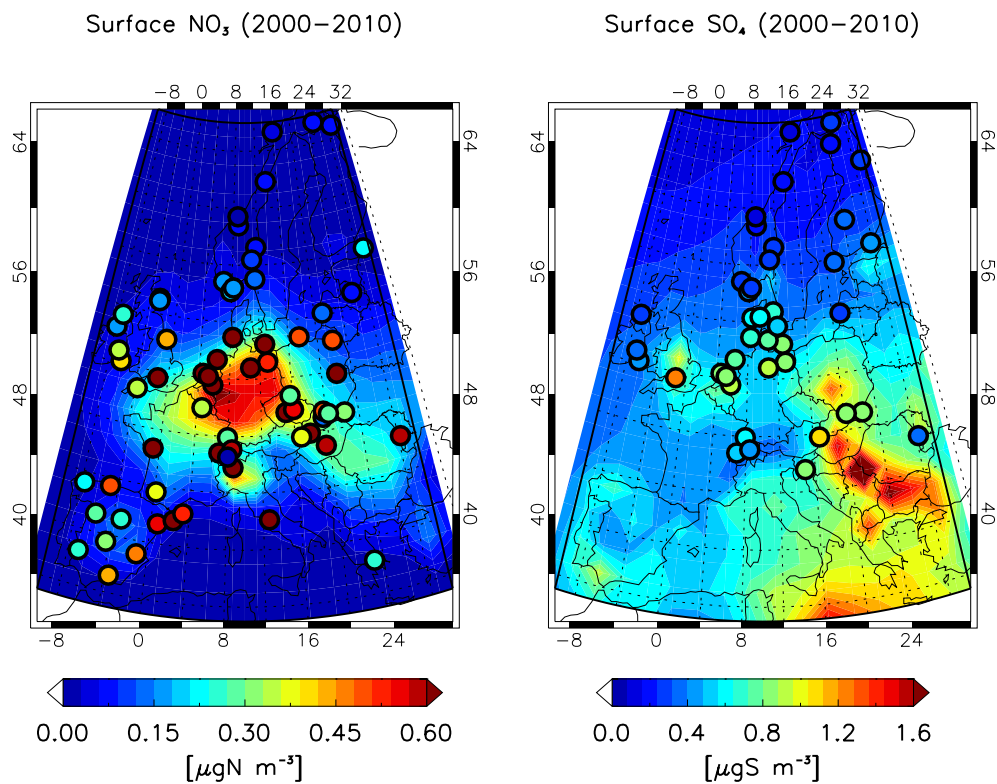
Figure 2. Mean nitrate (right panel) and sulfate (left panel) surface concentration (2000-2010) simulated by MATRIX-EQSAM overlaid by measurements from the EMEP network. The model data units match the units of the measured data ($\mu gX\ m^{-3}$ with X being N for nitrate and S for sulfate).

Atmospheric
Chemistry
and Physics
Discussions
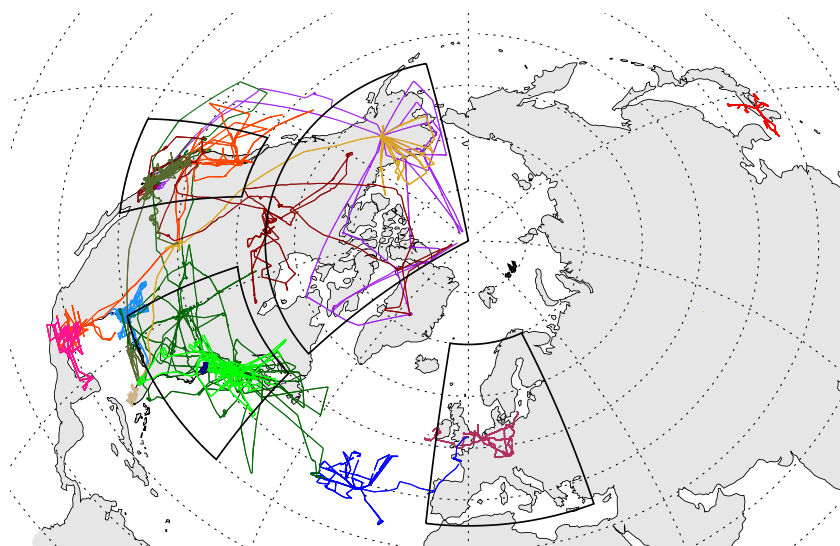
755

756   **Figure 3.** Flight tracks of 14 flight campaigns used in this study (2001-2011).

757

758

759

760

761

Atmospheric
Chemistry
and Physics
Discussions

762
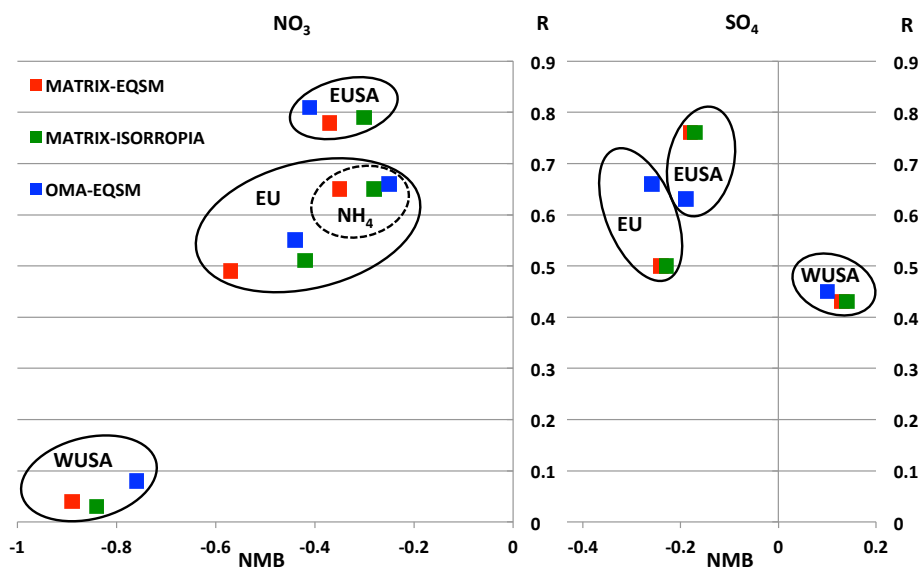
Figure 4. Surface regional statistics (2000-2010). Left panel: nitrate and ammonium (data
available only for EU); right panel: sulfate. The correlation coefficient (R) between the
simulation and the measurements is in the y-axis, and normalized mean bias (NMB) is in the x-
axis. MATRIX-EQSAM is in red, MATRIX-ISORROPIA II is in green and OMA-EQSAM is in blue.

767

Atmospheric
Chemistry
and Physics
Discussions

Surface EU (2000−2010)


768
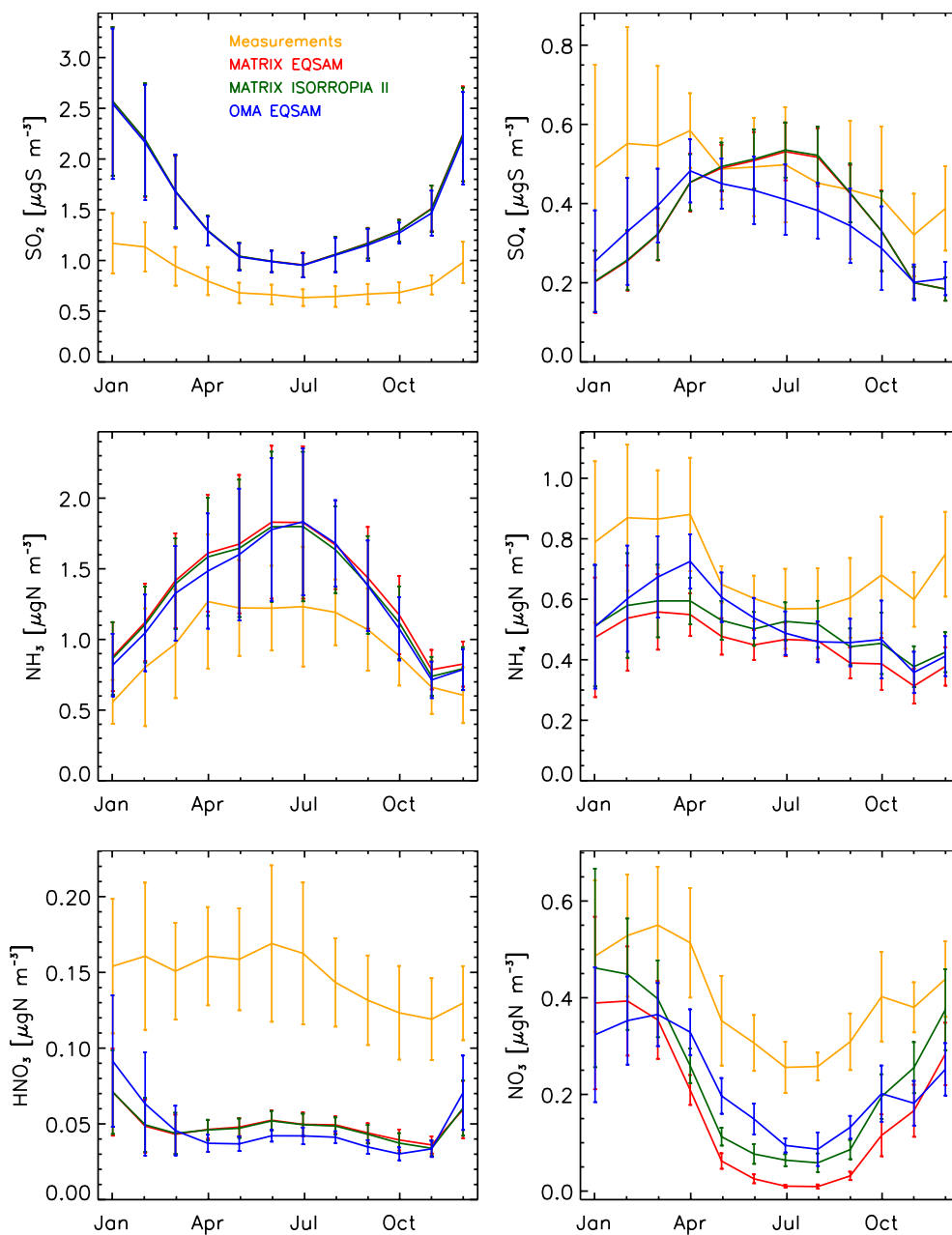
Figure 5. 2000-2010 mean annual cycle over Europe, error bars represent ± one standard
deviation. Measurements are in orange, MATRIX-EQSAM is in red, MATRIX-ISORROPIA II is in
green and OMA-EQSAM is in blue.

772
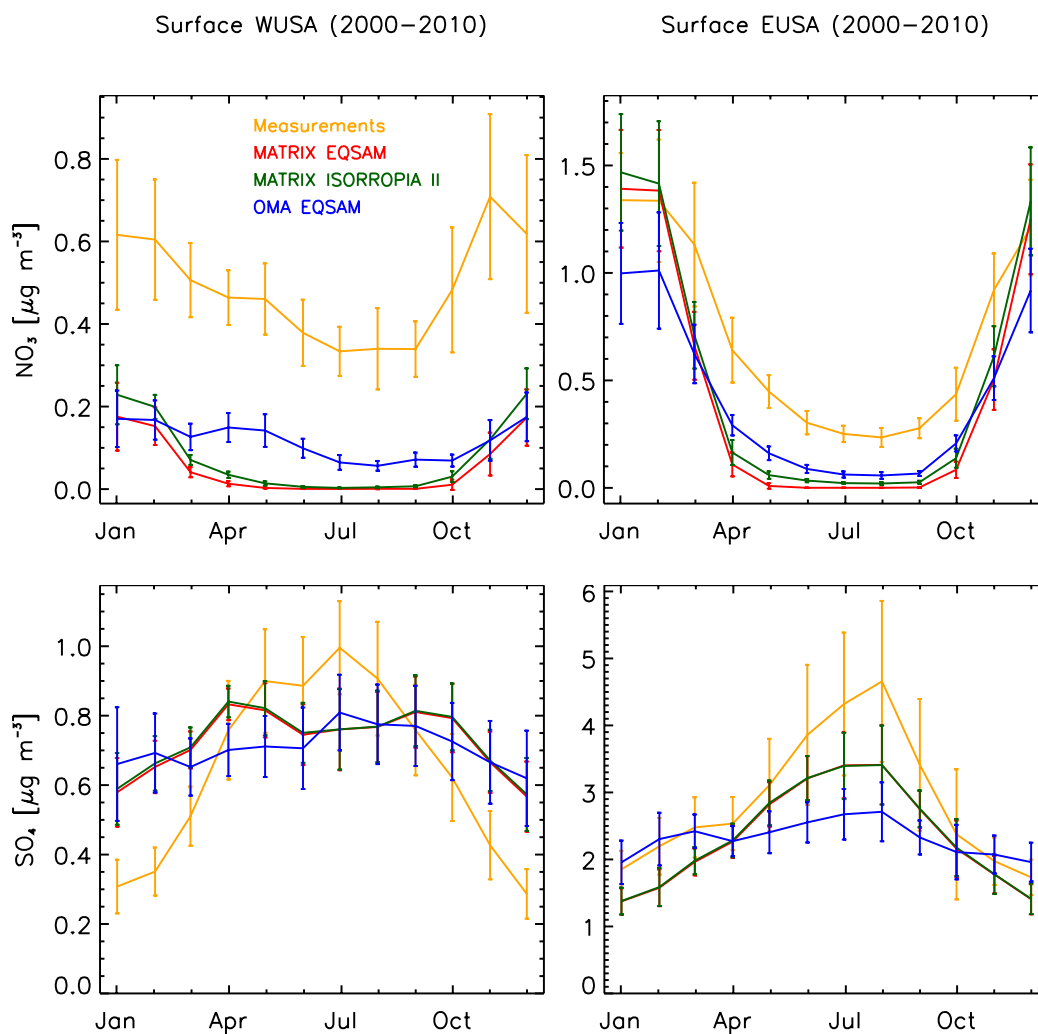
Figure 6. 2000-2010 mean annual cycle over WUSA (left) and EUSA (right), error bars represent
± one standard deviation. Measurements are in orange, MATRIX-EQSAM is in red, MATRIX-
ISORROPIA II is in green and OMA-EQSAM is in blue.

Atmospheric
Chemistry
and Physics
Discussions

Open Access

776
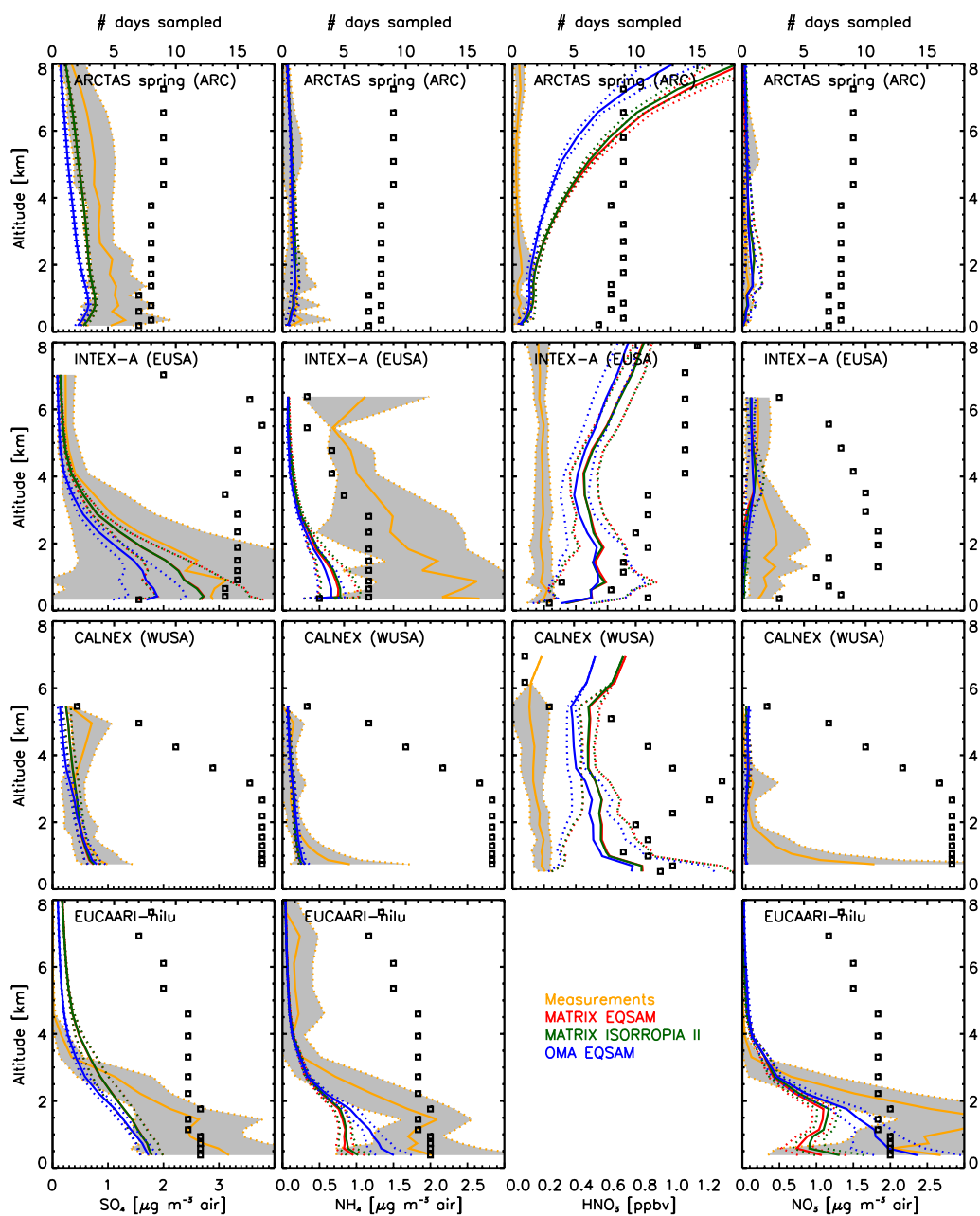
Figure 7. Mean regional concentration profiles from the arctic (first row), eastern USA (second
row), western USA (third row) and Europe (fourth row). First column is SO₄, second is NH₄, third
is HNO₃ and fourth is NO₃.

Atmospheric
Chemistry
and Physics
Discussions
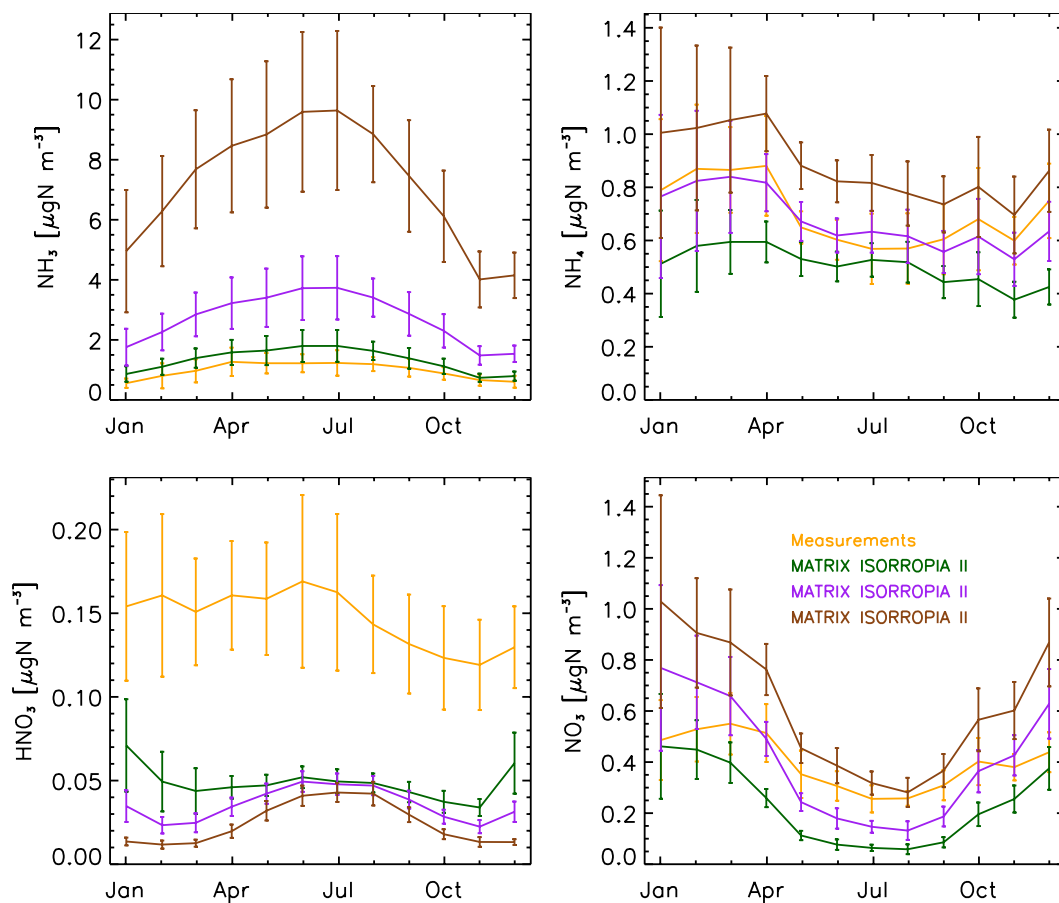
Figure 8. 2000-2010 mean annual cycle over Europe, error bars represent ± one standard
deviation. Measurements are in orange, MATRIX-ISORROPIA II: with regular emissions is in
green, with double agricultural NH_3 emissions is in purple, and with 5-times agricultural NH_3
emissions is in brown.

Atmospheric
Chemistry
and Physics
Discussions

Surface ratio EU (2000–2010)

785
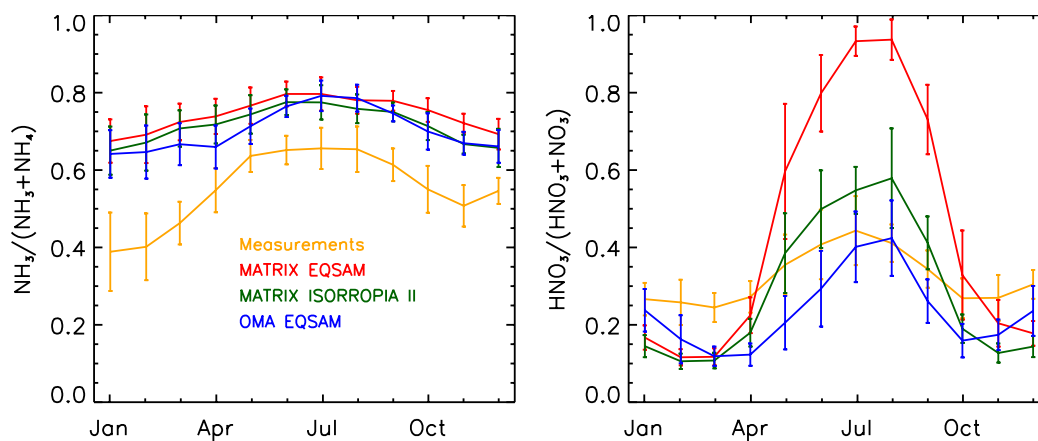
Figure 9. 2000-2010 mean partitioning ratio annul cycle over Europe, error bars represent ± one standard deviation. Measurements are in orange, MATRIX-EQSAM is in red, MATRIX-ISORROPIA II is in green and OMA-EQSAM is in blue.

789

Atmospheric
Chemistry
and Physics
Discussions

Open Access

790
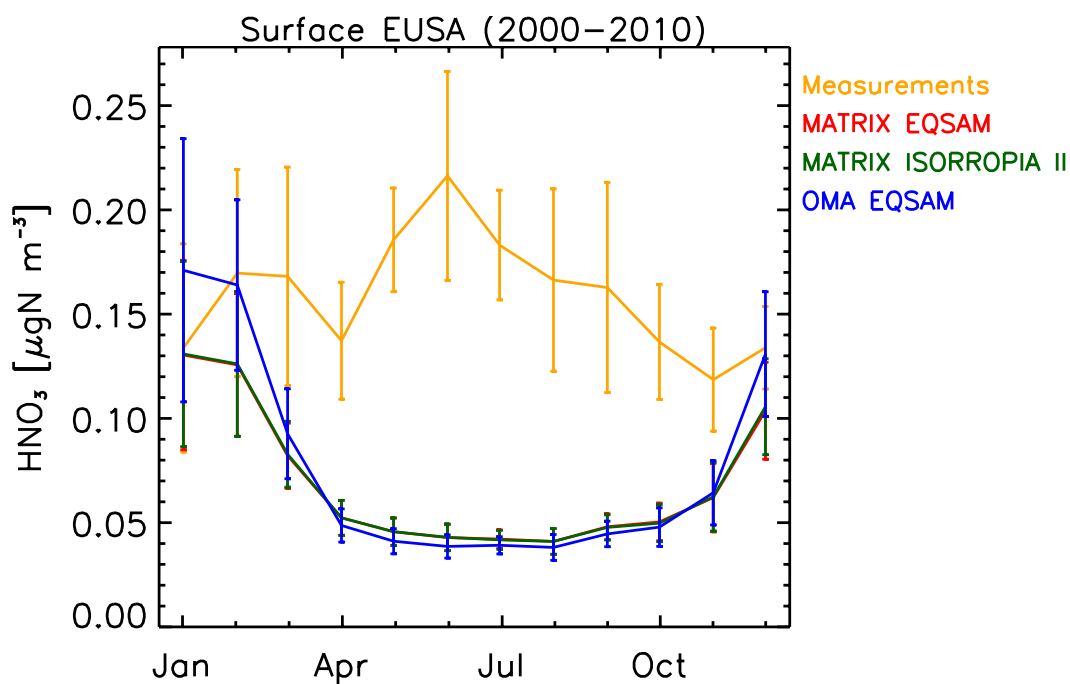
Figure A1. 2000-2010 HNO$_3$ mean annual cycle over EUSA (right), error bars represent ± one
standard deviation. Measurements are in orange, MATRIX-EQSAM is in red, MATRIX-ISORROPIA
II is in green and OMA-EQSAM is in blue.

Atmospheric
Chemistry
and Physics

Discussions

794
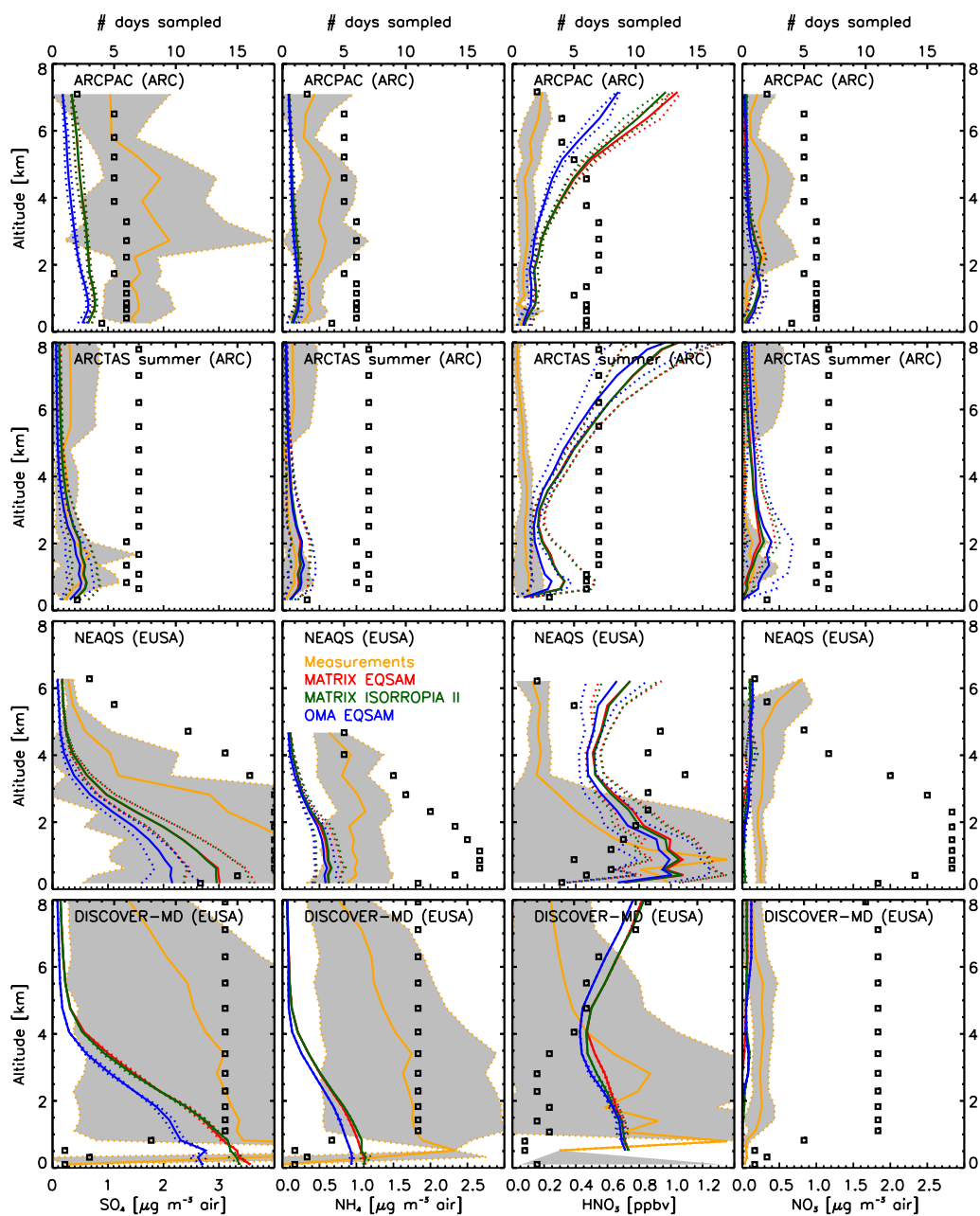
Figure A2. Mean regional concentration profiles. First column is SO_4, second is NH_4, third is HNO_3 and fourth is NO_3. Measurements are in orange, MATRIX-EQSAM is in red, MATRIX-ISORROPIA II is in green and OMA-EQSAM is in blue.

798

Atmospheric
Chemistry
and Physics
Discussions

Open Access

799

Figure A2: continued

Atmospheric
Chemistry
and Physics
Discussions


801
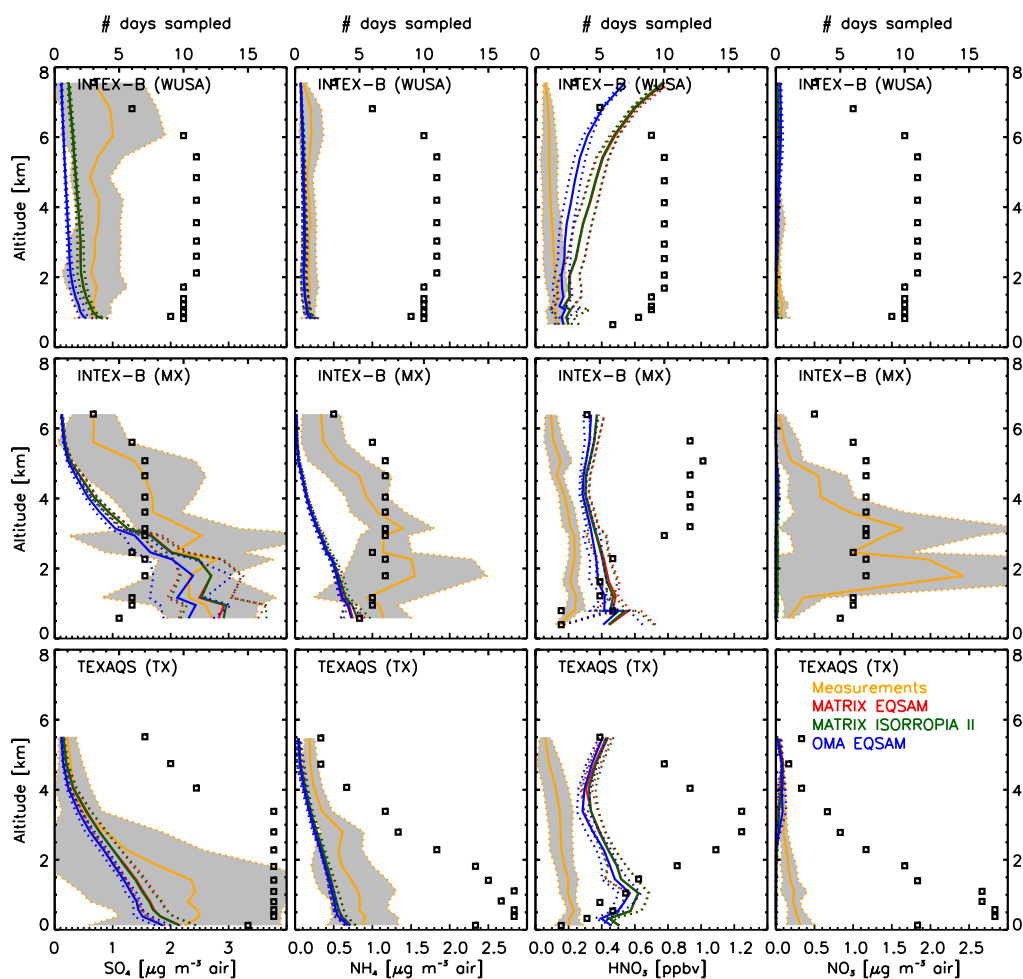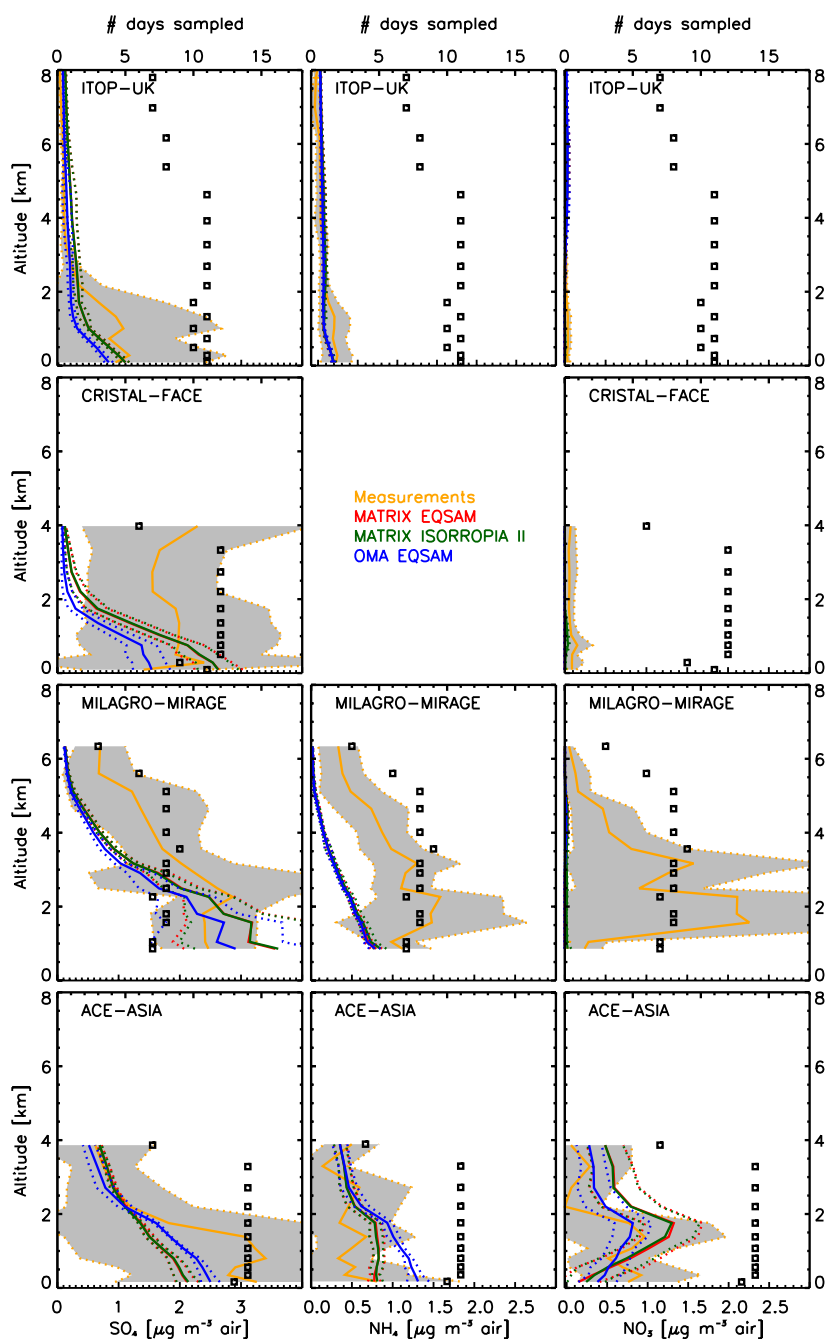
Figure A3. Mean regional concentration profiles. First column is SO_4, second is NH_4, and third is
NO_3. Measurements are in orange, MATRIX-EQSAM is in red, MATRIX-ISORROPIA II is in green
and OMA-EQSAM is in blue.

Atmospheric
Chemistry
and Physics
Discussions
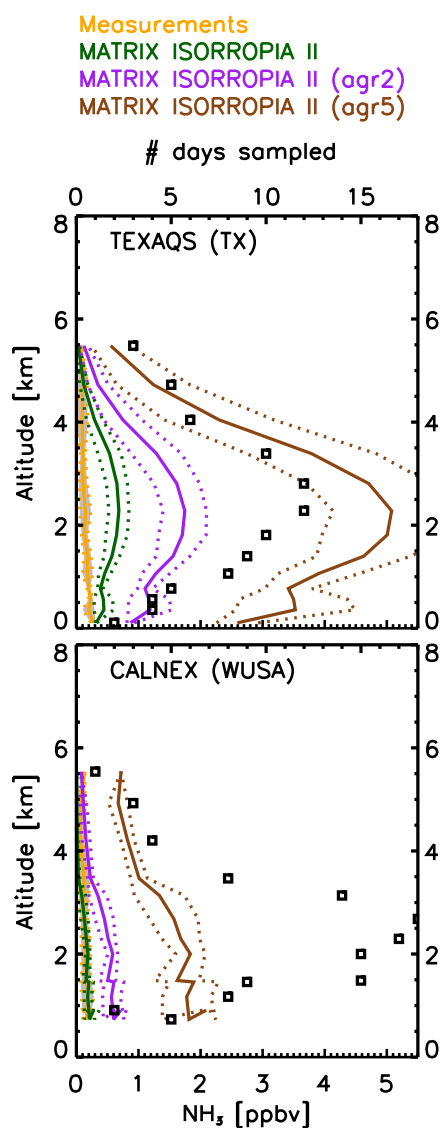
Figure A4. Mean regional NH$_3$ profiles from the TexAQS (upper panel) and CALNEX (lower panel) campaigns. Measurements are in orange, MATRIX-ISORROPIA II: with regular emissions is in green, with double agricultural NH$_3$ emissions is in purple, and with 5-times agricultural NH$_3$ emissions is in brown.

Atmospheric
Chemistry
and Physics
Discussions

Open Access
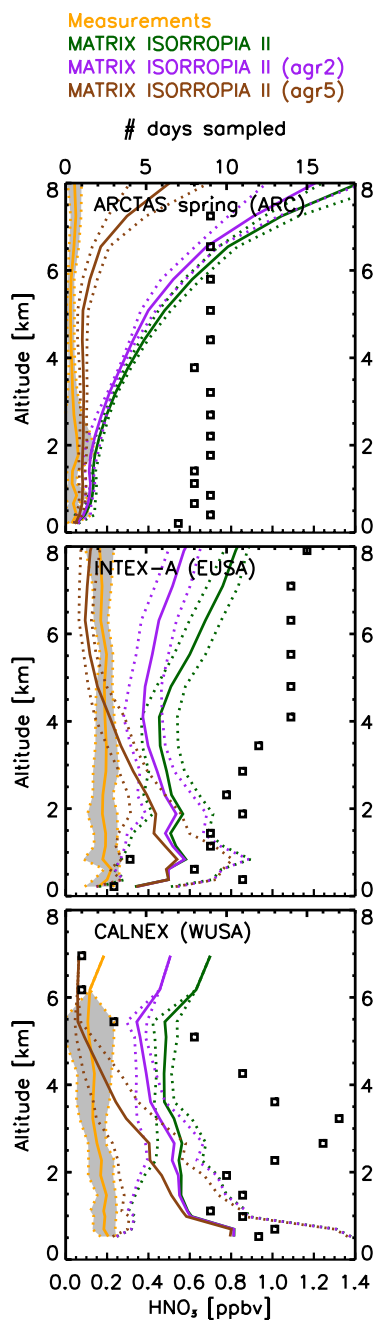
Figure A5. Mean regional HNO$_3$ profiles from the arctic, EUSA and WUSA. Measurements are in orange, MATRIX-ISORROPIA II: with regular emissions is in green, with double agricultural NH$_3$ emissions is in purple, and with 5-times agricultural NH$_3$ emissions is in brown.